Dymond MK. 2016 J. R. Soc. Interface 13: 20160228. http://dx.doi.org/10.1098/rsif.2016.0228

Received: 21 March 2016
Accepted: 25 July 2016

Mammalian phospholipid homeostasis: evidence that membrane curvature elastic stress drives homeoviscous adaptation *in vivo*

Marcus K. Dymond*[1]

[1]Division of Chemistry, School of Pharmacy and Biological Sciences, University of Brighton, BN2 4GL

*Author for correspondence: M.Dymond@brighton.ac.uk

Keywords: Data-driven modelling, lipid spontaneous curvature, intrinsic curvature hypothesis, homeoviscous adaptation, membrane order, membrane curvature elastic stress

Abstract

Several theories of phospholipid homeostasis have postulated that cells regulate the molecular composition of their bilayer membranes, such that a common biophysical membrane parameter is under homeostatic control. Two commonly cited theories are the intrinsic curvature hypothesis, which states that cells control membrane curvature elastic stress, and the theory of homeoviscous adaptation, which postulates cells control acyl chain packing order (membrane order). In this paper we present evidence from data-driven modelling studies that these two theories correlate *in vivo.* We estimate the curvature elastic stress of mammalian cells to be 4 – 7x10^{-12} N, a value high enough to suggest that in mammalian cells the preservation of membrane order arises through a mechanism where membrane curvature elastic stress is controlled.

These results emerge from analysing the molecular contribution of individual phospholipids to both membrane order and curvature elastic stress in nearly 500 cellular compositionally diverse lipidomes. Our model suggests the *de novo* synthesis of lipids is the dominant mechanism by which cells control curvature elastic stress and hence membrane order *in vivo*. These results also suggest cells can increase membrane curvature elastic stress disproportionately to membrane order by incorporating polyunsaturated fatty acids into lipids.

Dymond MK. 2016 J. R. Soc. Interface 13: 20160228. http://dx.doi.org/10.1098/rsif.2016.0228

Received: 21 March 2016
Accepted: 25 July 2016

1.0 Introduction

Theories of phospholipid homeostasis have arisen to explain long-standing observations that the steady-state phospholipid, cholesterol and protein composition of biological membranes changes in response to environmental conditions. For example chemicals, such as crude oil [1], PCB-153 [2], hydrocarbons, alcohols and detergents [3], fatty acids [4] and phospholipids [5], all cause changes to the lipid composition of biological membranes. Furthermore the effects of temperature on biomembrane lipid composition are well documented in large numbers of animal species such as in poikilotherms [6], Archaea [7], zooplankton [8], fish [9,10], mammals [11,12] and plants [13] as discussed [14,15]. Since it is well established in model membranes that different component lipids cause the collective lipid membrane to have different physical properties, the question 'which physical property are cells conserving in their biological membranes?' arises.

In answer to this question several theories have emerged. The theory of homeoviscous adaptation (HVA) suggests [16] that cells regulate the membrane order of their biological membranes, often described as regulation of membrane fluidity or membrane viscosity. In membranes order is quantified through an order parameter ranging from 0 (disorder) to 1 (order) and typically calculated using electron spin resonance or fluorescence anisotropy of probes such as diphenylhexatriene [9, 16]. The origin of HVA theory stems principally from the observations of Sinensky [16] who observed that the order parameter of *Escherichia coli* lipid membranes, determined by electron spin resonance, was unchanged despite the membranes having different lipid compositions at different temperatures. Over time a large number of other studies have shown that HVA, whilst initially formulated as a temperature-dependent response in bacteria, has a broader evolutionary significance [9,11]. For example, evidence suggests that membrane order is preserved by biological membranes in response to hydrostatic and osmotic pressure [10,17], low magnetic field strength [18] and chemicals [2,19], as discussed [14,15,20]. It has also become clear that lipids like cholesterol [21] play a critical role in regulating membrane order – or fluidity as it is commonly referred to in mammalian systems [22].

Received: 21 March 2016
Accepted: 25 July 2016

In contrast the intrinsic curvature hypothesis [23] states that the intrinsic (or spontaneous) curvature of biological membranes is tightly regulated through membrane compositional change, maintaining membrane curvature elastic energy [24,25] within tight boundaries. The origin of this theory stems from observations that cells appear to maintain their membrane composition away from a phase transition, so called homeophasic adaptation [26]. However, the fundamental observation that cells contain a large number of lipids that prefer to adopt curved non-bilayer structures led Gruner to postulate [23,27] that cells maintain the stored elastic energy that arises from curvature frustration constant. These are not the only theories of phospholipid homeostasis [28,29], for example it has been suggested that cells regulate the surface charge of their biological membranes by controlling the concentration of negatively charged lipids [30].

In a broader context, altered lipid compositions are associated with a number of diseases such as cancer [31], obesity [32], Alzheimer's disease [33], liver disease [34] and type 2 diabetes [35]. Therefore quantitative systems models of cellular phospholipid homeostasis are critical to understanding these pathologies.

1.1 Cellular mechanisms of phospholipid homeostasis

The mechanism through which the lipid biosynthetic network detects membrane biophysical properties, and adjusts biomembrane composition accordingly, is not well elucidated. Data suggest some of the enzymes involved in lipid biosynthesis, such as CTP:phosphocholine cytidylyltransferase (CCT) [36] and phospholipases [37,38], are regulated by membrane curvature elastic energy and could form part of a regulation pathway [39]. Membrane curvature elastic energy has also been implicated in the mechanism of action of some antineoplastic agents [40,41]. In contrast studies, using labelled spin probes for electron spin resonance [16] or membrane fluorescence depolarisation probes [9,11], have shown that membrane order in many biological membranes is preserved although membrane composition has changed [14,15,26]. There is evidence of the mechanism through which bacteria might control membrane order [42] but the precise pathways that eukaryotic cells use have not yet been discovered. However, Rho

Received: 21 March 2016
Accepted: 25 July 2016

signalling [43] and a group VIA Ca^{2+} independent-phospholipase-A_2 have been identified as significant [44]. Both biochemical and transcriptional mechanisms play a role in phospholipid homeostasis; in bacteria this is better understood than in eukaryotes [28]. The sterol regulatory element-binding proteins (SREBPs) are a critical part of the transcriptional mechanism of mammalian lipid homeostasis. SREBPs, in response to the levels of fatty acids in a membrane, proteolytically release fragments that enter the nucleus and activate some of the genes required for lipid homeostasis [45].

Previously we have identified two different ratio control mechanisms that operate in phospholipid homeostasis at the biochemical level. One of these was a ratio control mechanism for membrane disorder inspired by HVA [20] and the other was a ratio control mechanism derived from the intrinsic curvature hypothesis [46,47]. Both these studies used the lipidomes of HL60 and HeLa cells to construct a systems-level insight into the collective properties of cellular membranes through data-driven modelling, summarised in *section 1.2*.

1.2 Background: data-driven modelling with control functions in lipidomic datasets

The central premise of the data-driven approach is to state that all the different lipid compositions that exist across a cell line represent different combinations of lipids with an identical value of the common biophysical parameter (membrane order or membrane curvature elastic stress in these studies). If this premise is true, then the individual lipid concentrations multiplied by a factor that corresponds to their individual, structure-specific, contribution (w) to the common biophysical parameter must give rise to a mathematical function where one set of w values gives the lowest variance, in the numerical solution to that function, across all the lipidomic data sets. Critically the magnitude of this variance, which we express as a statistical coefficient of variance (c_v = 100% x (standard deviation/ mean)), validates the hypothesis. As a rule of thumb, under conditions where there is no reason to expect the control function to vary across a set of cell populations (such as in the case of asynchronous cell populations), we consider that a c_v of 10% or less suggests a control function is strongly evidenced. Whilst c_v values of between 10% and 20% demonstrate good evidence and c_v values greater than 20% demonstrate no evidence.

Received: 21 March 2016
Accepted: 25 July 2016

Mathematically we formulate each of the two hypotheses as ratio control functions; Eq. 1 shows the ratio control function inspired by HVA, where p_{dis} is in effect a proxy measure of membrane deviation from total order towards disorder.

$$p_{dis} = \frac{\sum_{n=0}^{b} w_{dis,n}[L_{dis,n}]}{\sum_{m=0}^{a} \frac{1}{w_{dis,m}}[L_{ord,m}]} \qquad \text{Eq. 1}$$

In formal terms Eq. 1 asks, given the set of all possible lipid species {*L*}, is there a universal pivot lipid species, L_{pdis}, that partitions *L* into subsets {L_{ord}+L_{pdis}}, {L_{dis}} such that the mean value of p_{dis}, has the minimum variance across multiple cell populations?

In Eq. 1 [$L_{dis,n}$] denotes the concentration of lipid (typically moles/ cell) that decreases membrane order, i.e. disordering lipids *n* and $(w_{dis})_n$ is the weighting factor for disorder for lipid *n.* Similarly [$L_{ord,m}$] is the concentration of lipid that increases order, i.e. ordering lipids *m* and $(w_{dis})_m$ is the weighting factor for disorder for lipid *m*. The variables *a* and *b* are the total numbers of ordering and disordering lipids respectively. We use a ratio control function because evidence has suggested that membrane order is regulated *in vivo* by the ratio of saturated to polyunsaturated fatty acids [11] present within the phospholipids constituting the cell membrane.

For the intrinsic curvature hypothesis we use the same conventional ratio control function but replace L_{dis} and L_{ord} with the terms L_{II} and L_0, where L_{II} is the concentration of type II lipids i.e. lipids that increase membrane stored elastic energy and L_0 is the concentration of type 0 lipids which decrease membrane stored elastic energy . We introduce the term p_{ces} as a proxy measure of membrane curvature elastic energy, calculated from Eq. 1 replacing w_{dis} with w_{ces}, which is the individual lipid weighting factor for curvature elastic stress. A ratio control function is used because it has been suggested that *in vivo* cells balance membrane stored elastic energy through controlling the ratio of type 0 to type II (or bilayer to non-bilayer forming lipids) [39].

Dymond MK. 2016 J. R. Soc. Interface 13: 20160228. http://dx.doi.org/10.1098/rsif.2016.0228

Received: 21 March 2016
Accepted: 25 July 2016

1.3 Background: quantifying membrane stored elastic energy

Critical to understanding this work is the quantification of membrane stored elastic energy from the lipid radius of spontaneous curvature (R_0) i.e. the unstressed radius of curvature of aggregated lipids. R_0 is typically derived from inverse hexagonal lyotropic liquid crystal phases by small angle X-ray scattering [38] and related to the elastic free energy of bending (ΔG_c) of a monolayer of surface area (A) by the Helfrich Hamiltonian [24], Eq. 2.

$$\Delta G_c = \tfrac{1}{2}\, \kappa_M A(c_1 + c_2 - 2c_0)^2 + \kappa_G A c_1 c_2 \qquad \text{Eq. 2,}$$

Where, c_1 (=1/R_1) and c_2 (=1/R_2) are the principal curvatures at the interface (with the convention that a monolayer with negative curvature curves towards water), c_0 (=1/R_0) is the intrinsic (or spontaneous) curvature of the monolayer, κ_M is the mean curvature bending rigidity and κ_G is the Gaussian curvature modulus.

Since it is not easy to obtain detailed information on the changing values of A, κ_M and κ_G for cells, we use curvature elastic stress (τ), Eq. 3, as a first order approximation of stored elastic energy.

$$\tau = -2\kappa_M c_0 \qquad \text{Eq. 3}$$

Extensive details of how the control functions were parameterised and how the values of w_{ces} and w_{dis} were obtained have been published previously [20,46], as summarised in *sections 2.1 to 2.3*. Figure 1 provides an overview of control mechanisms in phospholipid homeostasis and the importance of developing quantitative models to understand the role of lipids in health and the environment.

Dymond MK. 2016 J. R. Soc. Interface 13: 20160228. http://dx.doi.org/10.1098/rsif.2016.0228

Received: 21 March 2016
Accepted: 25 July 2016

1.4 Objectives

Our previous studies [20,46] gave two sets of coarse-grain parameters (w_{ces} and w_{dis}) determined by data-driven modelling using the HL60 and HeLa cell lipidomes. These w_{ces} and w_{dis} parameters can be substituted, with new lipidomic data, into Eq. 1 to give p_{dis} and p_{ces} values for these new lipidomes. Our first objective is to determine if the control functions and parameters determined previously are valid in these new lipidomic datasets. Secondly we evaluate the mechanisms by which both control functions might be maintained *in vivo*; a number of possibilities exist. There might, for example, be two separate control mechanisms, one for curvature elastic stress and one for membrane order. However, it is also possible that maintaining one of these membrane properties within tightly controlled boundaries automatically regulates the other membrane property, suggesting that membrane order and membrane curvature elastic stress are fundamentally entangled *in vivo*.

2.0 Materials and Methods

The lipidomes used in this study are derived from total cell extracts and have been published previously by various groups. Methodology through which control functions for membrane order [20] and the intrinsic curvature hypothesis [46] were parameterised is summarised in *sections 2.1 to 2.3*.

We have published lipidomes of the HL60, HL60 $_{oleate}$ (HL60 cells cultured in excess oleate), HeLa and HeLa $_{sync}$ (synchronised HeLa) cells [20,46,47]. The LDLR$_{mouse}$ lipidome was obtained from thioglycolate-stimulated wild-type and low-density lipoprotein receptor knockout (LDLR(-/-)) mice maintained on normal and Western (High-fat, high cholesterol) diets [48]. Lipidomes of RAW 264.7 cells cultured with KDO lipid-A (RAW 264.7$_{KDO}$), or compactin (RAW 264.7$_{compactin}$) or BMDM cells treated with compactin or ATP (BMDM $_{compactin}$ and BMDM $_{ATP}$, respectively) are freely available in the literature [48–50]. The

Received: 21 March 2016
Accepted: 25 July 2016

lipidomes of MDCK cells [51] and human brain cells exhibiting Alzheimer's Disease and control (NEURO $_{Alz}$) [52] are also available.

2.1 Assumptions in the data-driven modelling

To construct these data-driven models a number of assumptions have to be made, as discussed previously [20,46], which fall into two groups. The first group are assumptions about the experimental (lipidomic) data and ultimately determine the identity and diversity of the set of lipid species {L}. The second group are assumptions about the biophysics of the control mechanisms and dictate the form of the control function and how the *w* terms are constructed.

Assumptions deriving from the experimental data are that;

A) the lipid species (PC, PE, PS, PA, PI, DAG) used in the control functions represent greater than 90% of the total phospholipid composition of whole cells.
B) where isomeric or isobaric lipid species exist, all the lipids are assigned the dominant lipid identity.
C) the identity of lipid species can be assigned from the likely distribution of unsaturations, which is accomplished using the fatty acid species that predominate in mammalian cell lipidomes, i.e. the 14:0, 16:0, 16:1, 18:0, 18:1, 18:2, 18:3, 20:4, 20:5, 22:5, 22:6 fatty acids [53].

Assumption C is necessary because many of the lipidomes used in this study report at the lipid species level e.g. PC34:2, which does allow individual fatty acid chain lengths or the distribution of unsaturation to be assigned. In general, lipid identity assignments based upon the distribution of unsaturations are straightforward since, for example, PC 36:1 will contain 1 saturated chain and 1 monounsaturated chain (referred to as PC 0:1 in our models) and PC 36:2 will predominantly be PC 1: 1 rather than PC 0:2 (due to the greater predominance of the 18:1 fatty acid).

Dymond MK. 2016 J. R. Soc. Interface 13: 20160228. http://dx.doi.org/10.1098/rsif.2016.0228

Received: 21 March 2016
Accepted: 25 July 2016

Assumptions that dictate the form of the control functions and how the *w* terms are constructed are in part driven by the available lipidomic data but are also determined by current knowledge in membrane biophysics. These assumptions are that

D) the chain length of the individual fatty acid chains has no effect on membrane order or spontaneous curvature, which arises directly from assumption C.
E) control functions can be expressed as ratios where the individual lipids contribute to the collective numerator and denominator terms through ideal linear mixing.
F) curvature elastic stress increases with the number of lipid unsaturations and with lipid headgroup such that PS<PC<PI<PE<PA<DAG (for identical chain lengths), based on individual lipid contributions to membrane curvature elastic stress estimated from values of each lipid's spontaneous curvature [46].
G) membrane disorder increases with the number of lipid unsaturations and with lipid headgroup such that PA<PE<PS<PC<PI<DAG, ranked using *in vitro* trends in individual lipid T_m values, as discussed [20].

2.2 The origin of the terms w_{ces}, w_{dis} and pivot species (L_p)

The parameters w_{ces}, w_{dis} and pivot species (L_p) used to construct the control functions of the form shown in Eq. 1 were determined by a data-driven modelling approach using the HL60, HL60 $_{\text{oleate}}$ and HeLa lipidomes. According to a set of rules that stem from assumptions F and G, values of *w* were constructed by random iteration and used to calculate p_{dis} and p_{ces}. This approach was repeated using each lipid present in the HL60/HeLa lipidomes as the pivot lipid. The best sets of w_{ces} or w_{dis} and pivot species were selected as those that gave the lowest variance in p_{dis} or p_{ces} across all the cell populations [20,46] (reproduced in Tables S1 and S2).

2.*3 Determining the values of p_{dis} and p_{ces} for new lipidomes*

To calculate the values of p_{dis} and p_{ces} for each lipidome in this study, the individual concentrations of each lipid species (L) for each population of cells (i.e. each experimental

Received: 21 March 2016
Accepted: 25 July 2016

flask) were inputted into Eq. 1 along with the relevant value of w_{ces} *or* w_{dis} for that lipid species and control function (from Table S1 or S2). The mean average, standard deviation and coefficient of variance of p_{dis} and p_{ces} were then determined for each lipidome.

3.0 Results and Discussion

3.1 Control functions for membrane disorder and curvature elastic stress tested in new lipidomic data sets

The compositional abundance, statistical variance and origin of the lipidomes used in this study are shown in Table S3, which shows very clearly that there is significant diversity across the lipidomes studied. This is important to note since without this diversity our results are not a significant development on our previous studies. Table 1 shows p_{dis} and p_{ces}, their standard deviations and the c_v for each lipidomic dataset. A brief discussion of the effects of lipid composition on p_{ces} and p_{dis} is provided as supporting information, *section S1.1*.

In general, the magnitude of the c_v of p_{ces} and p_{dis} shown in Table 1 suggests that there is good evidence (since the c_v is generally below 20%) that the control functions, previously developed in the HL60 and HeLa cell lines, are in operation across these other mammalian lipidomes. Values of the mean p_{dis} and p_{ces} in Table 1 indicate that the trends we have previously reported [20,46] are also apparent in these wider datasets and that both properties are being regulated. For example individual cell lines have similar values of p_{dis}. Within error, the p_{dis} of BMDM $_{ATP}$ is 0.8 ± 0.2 and p_{dis} of BMDM $_{compactin}$ is 0.9 ± 0.2, the p_{dis} of RAW 264.7$_{compactin}$ cells is 0.6 ± 0.1, whilst the p_{dis} of RAW 264.7$_{KDO}$ cells is 0.6 ± 0.1. A similar trend is seen in the p_{ces} data as shown in Table 1. However the magnitude of p_{dis} and p_{ces} vary between cell lines indicating that the degree of membrane order and curvature elastic stress is likely to be different for each of the cell types.

Dymond MK. 2016 J. R. Soc. Interface 13: 20160228. http://dx.doi.org/10.1098/rsif.2016.0228

Received: 21 March 2016
Accepted: 25 July 2016

This larger set of data also suggests that the ratio of p_{dis} to p_{ces} for each cell line is around 3. This indicates a possible correlation between the two control functions across all the cell lines.

3.2 A strong correlation between p_{ces} and p_{dis} across all lipidomes and evidence of data clustering

A plot of p_{dis} versus p_{ces} for each individual population (*circa* 500) of cells was constructed and is shown in Figure 2A. Figure 2A suggests that there is a strong correlation between p_{dis} and p_{ces} *in vivo* (Pearson correlation coefficient of +0.93). This suggests there is an equally strong correlation between membrane curvature elastic stress and membrane disorder *in vivo*, such that as thermal disorder increases in the bilayer, curvature elastic stress also increases. In qualitative terms this makes sense since as temperature increases, increases in thermal disorder of the acyl chains will lead to a larger hydrocarbon chain cross-sectional area. This is turn leads to a tighter radius of curvature and greater curvature elastic stress in the bilayer arrangement. However, it is well established that the spontaneous curvature preference of individual lipids does not correlate with increased membrane disorder [54], suggesting a more complex mechanism is behind the correlation in Figure 2A and that this correlation is an emergent property of the mixture.

Another interesting observation is that for the cells analysed in Figure 2A p_{ces} and p_{dis} cluster over a range of 0.3 to 1.4 and 0.1 to 0.5 respectively. To get an idea of the range of values that p_{dis} and p_{ces} can have we used Eq. 1 to calculate p_{dis} and p_{ces} for binary lipid mixtures using the values of w_{ces} and w_{dis} in Tables S1 and S2. These data are shown in Figure 2B indicating that the p_{dis} and p_{ces} values for mammalian cells cluster when compared to the range of values possible.

Before exploring this relationship further it is worthwhile ensuring that the correlation between p_{dis} and p_{ces} is not artefactual. It is possible that the correlation might

Received: 21 March 2016
Accepted: 25 July 2016

occur due to the underlying lipid concentration, in which case any two control functions for p_{dis} and p_{ces} will show strong correlations because L, in Eq. 1, is significantly greater in magnitude than w. Therefore as a control measure, a similar analysis to that shown in Figure 2A was performed, where two, previously discarded w parameter sets (from our previous studies [20,46]) causing high variance (i.e. large c_v values) in p_{dis} and p_{ces} were plotted against each other. Figure S1 shows for the cellular lipidomes and Figure S2 shows for the binary lipid mixtures that in this instance p_{dis} and p_{ces} are poorly correlated.

3.3 Binary lipid studies of membrane order and curvature elastic stress explain the correlation between p_{ces} and p_{dis}

To the best of our knowledge only one literature study has proposed a quantitative model of the relationship between membrane order and lipid phase curvature [54]. Using binary lipid mixtures of 1-palmitoyl-2-oleoyl-*sn*-glycero-3-phosphocholine (POPC) and deuterated (d-31) 1-palmitoyl-2-oleoyl-*sn*-glycero-3-phosphoethanolamine (POPE), Lafleur et al. [54] determined the order parameter of both the inverse hexagonal (H_{II}) and fluid lamellar (L_α) phases at different lipid compositions. They found that the temperature dependence of the membrane order parameter follows the same quantitative relationship in both phases but also that the membrane order parameter scales as a function of the curvature of the lipid mixture. This suggests that there are two components that drive membrane order, the first component is thermal energy and the second is stored elastic energy. Lafleur et al. [54] show that the average membrane order parameter of POPE:POPC 82:18 in the L_α phase ($S_{L\alpha}$) is *circa* 0.2 and in the H_{II} phase (S_{HII}) is *circa* 0.08 (both at 30°C). In fact over the composition range studied, order in the L_α phase is 2 to 3 times greater than in the H_{II} phase, at all temperatures. Thus in the bilayer phase the effects of thermal disorder are attenuated by the frustration of lipid spontaneous curvature.

If we consider the case for mammalian cells (at constant temperature) then, since there is evidence to suggest curvature elastic stress is tightly regulated, the results of Lafleur et al.[54] imply that the attenuation of thermal order must also be constant. Furthermore if the thermal contribution to membrane order is significantly bigger than the contribution

Received: 21 March 2016
Accepted: 25 July 2016

from curvature elastic stress *in vivo* then controlling curvature elastic stress will have little effect on net membrane order. Therefore membrane order would need to be independently regulated. Similarly, if the thermal contribution to membrane order *in vivo* is significantly lower than the contribution from curvature elastic stress then, to regulate membrane order, it is theoretically only necessary to regulate curvature elastic stress. To develop this analysis further it is necessary to estimate the curvature elastic stress of the cellular membranes in this study.

3.4 Estimating curvature elastic stress and the ratio $S_{L\alpha}$ /S_{HII} in vivo

There are no *in vivo* measurements of the spontaneous curvature, curvature elastic stress or stored elastic energy of biological membranes reported in the literature. Therefore the best estimate of the magnitude of curvature elastic stress *in vivo* comes from calibrating p_{ces} against the calculated curvature elastic stress present in binary mixtures of lipids. If we compare this estimate of curvature elastic stress in a cell membrane to the curvature elastic stress in lipid mixtures with published values of the ratio $S_{L\alpha}$ /S_{HII} we can estimate the ratio $S_{L\alpha}$ /S_{HII} *in vivo*.

Figure 3A shows curvature elastic stress (τ), see Eq.3, versus p_{ces} for two binary lipid mixtures of DOPE (R_0 = -28.5 Å [55]) and POPC (R_0 = -454.5 Å) [56], and DOG (R_0 = -11.5 Å [55]) and POPC. (method shown in *section S1.2*). The values of p_{ces} in Table 1 range from 0.15 to 0.38. According to Figure 3A, and assuming that this binary lipid model is valid for the lipidomes studied, then τ in these biological membranes is around 4 - 7x10^{-12} N. Figure 3B shows the relationship between τ and $S_{L\alpha}$ /S_{HII} in model membranes, calculated from the data of Lafleur et al. [54]. From Figure 3B it is clear that at this value of τ, $S_{L\alpha}$ /S_{HII} is around 2.6 and hence τ will have a dominating effect on membrane order in these cells.

3.5 A mechanism for phospholipid homeostasis: curvature elastic stress drives membrane order in mammalian cells

Received: 21 March 2016
Accepted: 25 July 2016

A ratio of $S_{L\alpha}$ /S_{HII} = 2.6 is consistent with a mechanism where, at constant temperature, the regulation of membrane order *in vivo* could be accomplished by regulation of τ. However Lafleur et al. [54] also present data to show that in the same POPE and POPC binary lipid systems where $S_{L\alpha}$ /S_{HII} ranges from 2.6 to 3.11 the absolute magnitude of the orientational order parameter does not change significantly with lipid composition and hence τ. An explanation of this stems from Figure 3B, where $S_{L\alpha}$ /S_{HII} appears to plateau at values of 3 over the range studied. In this regime the effect of changes in τ on absolute order will be small, assuming constant temperature, possibly because the system is highly stressed. This in turn suggests that if mammalian cells maintain τ at around 2 x10^{-11} N or above, $S_{L\alpha}$ /S_{HII} will be about 3 and absolute membrane order will be constant. However, this does assume that the non-linear curve fitted to Figure 3B is appropriate. Assuming it is valid, then the lower value of $S_{L\alpha}$ /S_{HII} = 2.6, which is at the steepest point in the curve, suggests membrane order will be more sensitive to τ in this regime. It is however worth noting that the effect of protein is ignored in the calculation of τ. Theoretically $\bar{\kappa}_M$ will increase with increasing protein content in the lipid bilayer as discussed [57], therefore it is likely that the estimated value of τ *in vivo* is at the lower extreme of the real value.

This mechanism explains why lipids such as cholesterol have an ordering effect on the other lipids present in biological membranes [58]. The radius of spontaneous curvature of cholesterol is tightly negative (R_0 = -20 Å) [56] and hence in a bilayer arrangement, frustration of the spontaneous curvature of cholesterol is one mechanism through which membrane order might be controlled. This suggests that other lipids with negative spontaneous curvature will also increase membrane order when their curvature is frustrated, as a recent *in vivo* study that replaces cholesterol with PE indicates [59].

It is interesting to ask whether the same mechanism might operate to maintain membrane order in cells constant at different temperatures. Since $S_{L\alpha}$ /S_{HII} is around 2.6 to 3 at all temperatures studied by Lafleur et al. [54] (from 20°C to 80°C) then it is possible that by regulating τ in response to temperature change, membrane order will also be regulated. However, given that we have estimated τ in mammalian cells at constant temperature, further work will need to be carried out to assess this.

Dymond MK. 2016 J. R. Soc. Interface 13: 20160228. http://dx.doi.org/10.1098/rsif.2016.0228

Received: 21 March 2016
Accepted: 25 July 2016

3.6 Mechanistic insights into the correlation between membrane curvature elastic stress and membrane order in vivo

To understand how the individual lipid species contribute to both p_{ces} and p_{dis} we looked at how hypothetical lipid compositional changes would simultaneously affect both terms. This was achieved by normalising the difference in magnitude of *w* between each lipid and each pivot lipid species i.e. $(w_{ces\ Lp} - w_{ces\ L})/\ w_{ces\ Lp}$ or $(w_{dis\ Lp} - w_{dis\ L})/\ w_{dis\ Lp}$ for the set of lipids {L}. Figure 4 shows the resultant plot restricted to the lipid species that have the greatest impact on the control functions (PC, PE, PS and PI headgroups) [20,46,47]. Compositional changes in the lipid species that fall on the dashed diagonal line in Figure 4A to C will change the values of p_{dis} and p_{ces} by equal amounts for a single cell population. Figures 4A to 4C show very clearly that a compositional change in any of the individual lipid species (lipid headgroup classes are shown in Figure 4A, unsaturation combinations are shown in Figure 4B) will not increase p_{dis} more than p_{ces}, since none of the lipids appear above the diagonal line. Biologically Figure 4B shows that disorder i.e. p_{dis} does not increase linearly with unsaturation. This is to be expected, since once a single unsaturation has been added, further unsaturations allow the chains to adopt some more ordered *gauche* conformations as well as less ordered conformations [14]. Furthermore two groups of lipids can be defined as shown in Figure 4C, *Group 1 (*subdivided into *1a* and *1b)* and *Group 2*;

- *Group 1* lipids fall on the line of equality (or close to it) and thus compositional increases in these lipids decrease (*Group 1a*) or increase (*Group 1b*) the magnitude of p_{ces} and p_{dis} more or less equally.
- *Group 1a* lipids are saturated lipids of all headgroups e.g. PC, PS, PE and PI (see Figures 4A and B).
- *Group 1b* lipids are comprised of mono, di and triunsaturates of PC, PS, PE and PI (see Figures 4A and B).
- *Group 2* lipids are a significant distance from the line of equality and compositional increases in these lipids increase the magnitude of p_{ces} to a greater extent than p_{dis}.
- *Group 2* lipids are comprised of polyunsaturates e.g. 20:4 and 22:6 containing lipids with PC, PS, PE and PI headgroups (see Figures 4A and B).

Received: 21 March 2016
Accepted: 25 July 2016

This information allows us to understand, mathematically, how the correlation between the p_{dis} and p_{ces}, Figure 2A, is maintained *in vivo*, since the most compositionally abundant lipids in each lipidome (Table S3) are in *Groups 1a* and *1b*.

3.7 *Group 1 and Group 2 lipids have different biosynthetic pathways*

Interestingly Figure 4B suggests that the polyunsaturated lipids in *Group 2* might drive underlying variation in the ratio of p_{dis} to p_{ces}. This is an interesting observation when the different biosynthetic routes for lipid production are considered. *In vivo* biosynthesis of lipids occurs through two pathways. Phospholipids are synthesised *de novo* through the Kennedy pathway [60], from free fatty acids via diacylglycerols, or by fatty acid remodelling through the Lands cycle [61]. The polyunsaturated fatty acids 20:4, 20:5 and 22:6 appear to be exclusively substituted into lipids through fatty acid remodelling [62]. What is striking about Figure 4C is that the lipids in *Groups 1*a and *1b* are exclusively synthesised by the *de novo* route and the lipids in *Group 2* are all synthesised by the remodelling route. This suggests a cellular mechanism through which membrane curvature elastic stress could be varied disproportionately to membrane order *in vivo.* This process would occur via the Lands cycle, where lipids are switched between *Group 1* and *2* by exchange of a 20:4, 20:5 or 22:6 fatty acid with one of the fatty acids on a G*roup 1* lipid.

3.8 Evidence that Group 2 lipids drive cell cycle variations in membrane order and curvature elastic stress

In other work [47] we concluded that for HeLa cells curvature elastic stress increases in the Gap 2/ Mitosis (G2/M) phase of the cell cycle. We concluded that this is the result of increases in arachidonic acid containing lipids. In particular we identified PC18:1/20:4, PE 18:0/20:4, PE 18:1/20:4, PE 18:0/20:4, PI 18:1/20:4, PI 18:0/20:4 and PS 18:0/20: 4, which are in *Group 2* as identified in this work. Furthermore, we observed a fall in curvature elastic stress in S phase due to an increase in saturated and monounsaturated lipids with PC, PE, PS and PI headgroups, which are in G*roup 1*. Figure 4D shows a reconstruction of the original

Received: 21 March 2016
Accepted: 25 July 2016

plots of p_{dis} and p_{ces} for the HeLa cell cycle normalised to their first time point. This analysis allows us to look at the relative magnitude of curvature elastic stress and membrane order as they vary about the cell cycle. Initially p_{dis} and p_{ces} drop in proportion with each other before there is a rise in p_{ces} that is greater than the rise in p_{dis} at 12 hours. What is now clear is that the difference in p_{ces} and p_{dis} at 12 hours (G2/M) is clearly due to the elevated *Group 2* polyunsaturated lipids.

Using transcriptomic data in the NCBI GEO database for HeLa cells as they traverse the cell cycle [63] we looked for evidence to suggest that any of the acyltransferase enzymes [62] that perform polyunsaturated fatty acid substitutions, full list shown in Table S4, were expressed to a greater extent as cell moved into the G2/ M phase of the cell cycle. We could find no transcriptional correlation, suggesting a biochemical or post-translational mechanism drives substitution with polyunsaturated fatty acids. Many of the acyltransferase enzymes that substitute polyunsaturated fatty acids are membrane spanning [62] therefore the likely regulatory mechanism is through membrane curvature elastic energy as demonstrated for several other intrinsic proteins [38]. However, it is also possible that membrane order might be being sensed, as is thought to occur in bacterial membranes through the so-termed 'sunken-buoy' motif [42] in some transmembrane proteins.

4.0 Conclusions

4.1 Limitations, assumptions and the development of better data-driven models

In this work a number of assumptions are made as discussed in *section 2.1*. It is useful to consider the impact of these assumptions on the conclusions of this study. The need for these assumptions partly stems from the current limitations of lipidomic analyses, as summarised in Figure 5 and below.

i) Lipidomic analyses are mass spectrometric and some lipid structural information such as fatty acid chain length, position and distribution of unsaturations (critical

Received: 21 March 2016
Accepted: 25 July 2016

to efficient biophysical parameterisation) is lost due to isomerism (Assumptions A, B & C).

ii) Lipidomic datasets are predominantly obtained from total lipid extracts and contain no information on cellular lipid spatial heterogeneity. In particular, subcellular lipid distribution, membrane protein composition, lipid microdomain composition and lipid leaflet compositional asymmetry are lost.

The limitations presented in point (i) are likely to be overcome with new methodological developments in lipid mass spectrometry. This will enable a less coarse-grained approach to data-driven modelling to be performed by allowing a greater number of lipid species to be identified and included in the models. We know, however, from previous work [20] that the most compositionally abundant lipids (typically PC and PE lipids) dominate the control functions and since these are already included in the model the inclusion of less abundant lipids is unlikely to impact the conclusions of this manuscript.

The limitations presented in point (ii) will be overcome by new methods of lipid extraction and membrane fractionation. This will enable control functions to be determined for individual subcellular membranes. If all the membranes, domains and membrane leaflets in the cell have the same magnitudes of p_{ces} and p_{dis} then this will be of no consequence, however there is no reason to expect this. Furthermore quantitative details of the membrane proteome obtained under the same conditions as the lipidome will enable the set of total membrane proteins $\{P_M\}$ to be included in control functions. This is important since some membrane proteins can mitigate lipid curvature effects hence their inclusion will lead to more accurate models.

Control functions are parameterised as a mixture where the components contribute linearly as a function of concentration to the mixture properties (assumption E). The use of this principle of ideal mixing is widespread [25,36,54,55] in the biophysics community and unlikely to be re-evaluated. Related to this is the low data density of the relevant lipid biophysical data, which allows the ranking of lipid contributions to curvature elastic stress (assumption F) or membrane order (assumption G). As new data emerge, a less coarse-

Received: 21 March 2016
Accepted: 25 July 2016

grained approach to generate the values of w_{ces} and w_{dis} can be employed. However, since the major trends are well established it is unlikely that either assumption E or F is likely to be re-evaluated.

4.2 Summary of key results and future directions

Using data-driven models [20,46] as proxies for membrane disorder and membrane curvature elastic stress *in vivo* we have analysed the lipidomes of *circa* 500 cellular populations. Our analysis suggests;

- Both p_{ces} and p_{dis} are well-evidenced in the new data sets,
- a positive correlation (R = + 0.93) between the two control functions across the new lipidomes,
- curvature elastic stress in mammalian cells is *circa* 4 - 7x10^{-13} N
- regulation of membrane order (membrane fluidity/ viscosity) can be achieved by regulation of membrane curvature elastic stress but not vice versa.
- lipids synthesised through the Kennedy pathway have a more or less equal effect on both control functions,
- Lands' cycle offers a route by which cells might increase curvature elastic stress to a greater extent than membrane order.

These findings have several implications for model studies of lipid protein interactions. For example it is common practice to look at the activity of membrane interacting proteins in binary lipid mixtures. Focusing model membrane studies on lipid mixtures with p_{dis} and p_{ces} values comparable to those in real cells might reveal new insights into how lipid composition affects protein activity, particularly if p_{ces} and p_{dis} values are used to normalise protein activity in across lipid compositions.

These data-driven models present a number of hypotheses which ought to be tested independently. There are a number of challenges that currently prevent this. The biggest is that there is currently no way to directly measure stored elastic energy in a membrane.

Received: 21 March 2016
Accepted: 25 July 2016

Rather its magnitude must be inferred using the intrinsic parameters of lipid mixtures and linear mixing. Membrane order can be measured in membranes; hence one approach to test the hypotheses presented is to measure membrane order and compare it to the calculated curvature elastic energy in complex lipid mixtures. The relatively few spontaneous curvatures values of lipids in the literature, when compared to the number of lipids in cells, currently prevent this analysis.

Data accessibility

This manuscript makes use of primary open access data that has previously been published; all relevant data and their source are cited at the appropriate point in the text.

Competing interests

The author declares no competing interests.

Acknowledgements

The author acknowledges Lisa O'Rourke for proofreading drafts of this manuscript and George S. Attard for helpful discussions.

Received: 21 March 2016
Accepted: 25 July 2016

References

1. Mazzella, N., Syakti, A. D., Molinet, J., Gilewicz, M., Doumenq, P., Artaud, J. & Bertrand, J.-C. 2005 Effects of crude oil on phospholipid fatty acid compositions of marine hydrocarbon degraders: estimation of the bacterial membrane fluidity. *Environ. Res.* **97**, 300–311. (doi:10.1016/j.envres.2004.06.007)
2. Gonzalez, A., Odjélé, A. & Weber, J.-M. 2013 PCB-153 and temperature cause restructuring of goldfish membranes: Homeoviscous response to a chemical fluidiser. *Aquat. Toxicol.* **144-145**, 11–18. (doi:10.1016/j.aquatox.2013.09.018)
3. Wieslander, Å., Rilfors, L. & Lindblom, G. 1986 Metabolic changes of membrane lipid composition in Acholeplasma laidlawii by hydrocarbons, alcohols, and detergents: arguments for effects on lipid packing. *Biochemistry* **25**, 7511–7.
4. King, M. E. & Spector, A. A. 1978 Effect of specific fatty acyl enrichments on membrane physical properties detected with a spin label probe . *J. Biol. Chem.* **253**, 6493–6501.
5. Ferguson, K. A., Glaser, M., Bayer, W. H. & Vagelos, P. R. 1975 Alteration of fatty acid composition of LM cells by lipid supplementation and temperature. *Biochemistry* **14**, 146–51.
6. Guschina, I. A. & Harwood, J. L. 2006 Mechanisms of temperature adaptation in poikilotherms. *FEBS Lett.* **580**, 5477–5483. (doi:10.1016/j.febslet.2006.06.066)
7. Oger, P. M. & Cario, A. 2013 Adaptation of the membrane in Archaea. *Biophys. Chem.* **183**, 42–56. (doi:10.1016/j.bpc.2013.06.020)
8. Gladyshev, M. I. et al. 2011 Effect of temperature on contents of essential highly unsaturated fatty acids in freshwater zooplankton. *Limnol. - Ecol. Manag. Inl. Waters* **41**, 339–347. (doi:10.1016/j.limno.2011.03.001)
9. Behan-Martin, M. K., Jones, G. R., Bowler, K. & Cossins, A. R. 1993 A near perfect temperature adaptation of bilayer order in vertebrate brain membranes. *Biochim. Biophys. Acta - Biomembr.* **1151**, 216–222. (doi:10.1016/0005-2736(93)90106-A)
10. Behan, M. K., Macdonald, A. G., Jones, G. R. & Cossins, A. R. 1992 Homeoviscous adaptation under pressure: the pressure dependence of membrane order in brain myelin membranes of deep-sea fish. *Biochim. Biophys. Acta - Biomembr.* **1103**, 317–323. (doi:10.1016/0005-2736(92)90102-R)
11. Cossins, A. R. & Prosser, C. L. 1978 Evolutionary adaptation of membranes to temperature. *Proc. Natl. Acad. Sci. U. S. A.* **75**, 2040–2043.
12. Anderson, R. L., Minton, K. W., Li, G. C. & Hahn, G. M. 1981 Temperature-induced homeoviscous adaptation of chinese hamster ovary cells. *Biochim. Biophys. Acta - Biomembr.* **641**, 334–348. (doi:10.1016/0005-2736(81)90490-9)
13. Davy De Virville, J. et al. 2002 Homeoviscous and functional adaptations of mitochondrial membranes to growth temperature in soybean seedlings. *Plant, Cell Environ.* **25**, 1289–1297. (doi:10.1046/j.1365-3040.2002.00901.x)

Received: 21 March 2016
Accepted: 25 July 2016

14. Hazel, J. R. 1995 Thermal adaptation in biological membranes: is homeoviscous adaptation the explanation? *Annu. Rev. Physiol.* **57**, 19–42. (doi:10.1146/annurev.ph.57.030195.000315)

15. Hazel, J. R. 1997 'Thermal Adaptation in biological membranes: beyond homeoviscous adaptation.' *Adv. Mol. cell Biol.* **19**, 57–102.

16. Sinensky, M. 1974 Homeoviscous adaptation-a homeostatic process that regulates the viscosity of membrane lipids in Escherichia coli. *Proc. Natl. Acad. Sci. U. S. A.* **71**, 522–525.

17. Laroche, C., Beney, L., Marechal, P. A. & Gervais, P. 2001 The effect of osmotic pressure on the membrane fluidity of Saccharomyces cerevisiae at different physiological temperatures. *Appl. Microbiol. Biotechnol.* **56**, 249–254. (doi:10.1007/s002530000583)

18. Santoro, N., Lisi, A., Pozzi, D., Pasquali, E., Serafino, A. & Grimaldi, S. 1997 Effect of extremely low frequency (ELF) magnetic field exposure on morphological and biophysical properties of human lymphoid cell line (Raji). *Biochem. Biophys. Acta* **1357**, 281–290.

19. Rybczynska, M., Spitaler, M., Knebel, N. G., Boeck, G., Grunicke, H. & Hofmann, J. 2001 Effects of miltefosine on various biochemical parameters in a panel of tumor cell lines with different sensitivities. *Biochem. Pharmacol.* **62**, 765–772. (doi:10.1016/S0006-2952(01)00715-8)

20. Dymond, M. K. 2015 Mammalian phospholipid homeostasis: Homeoviscous adaptation deconstructed by lipidomic data-driven modelling. *Chem. Phys. Lipids* **191**, 136–146. (doi:10.1016/j.chemphyslip.2015.09.003)

21. Crockett, E. L. & Hazel, J. R. 1995 Cholesterol levels explain inverse compensation of membrane order in brush border but not homeoviscous adaptation in basolateral membranes from the intestinal epithelia of rainbow trout. *J. Exp. Biol.* **198**, 1105–1113.

22. Yu, Y., Vidalino, L., Anesi, A., Macchi, P. & Guella, G. 2014 A lipidomics investigation of the induced hypoxia stress on HeLa cells by using MS and NMR techniques. *Mol. Biosyst.* **10**, 878–890. (doi:10.1039/c3mb70540d)

23. Gruner, S. M. 1985 Intrinsic curvature hypothesis for biomembrane lipid composition: a role for nonbilayer lipids. *Proc. Natl. Acad. Sci. U. S. A.* **82**, 3665–3669.

24. Helfrich, W. 1973 Elastic properties of lipid bilayers: theory and possible experiments. *Z. Naturforsch. C.* **28**, 693–703. (doi:10.1002/mus.880040211)

25. Seddon, J. M. 1990 Structure of the inverted hexangonal (HII) phase, and non-lamellar phase-transitions of lipids. *Biochim. Biophys. Acta* **1031**, 1–69.

26. Vigh, L., Maresca, B. & Harwood, J. L. 1998 Does the membrane's physical state control the expression of heat shock and other genes? *Trends Biochem. Sci.* **10**, 369–374.

27. Österberg, F., Rilfors, L., Wieslander, Å., Lindblom, G. & Gruner, S. M. 1995 Lipid

Received: 21 March 2016
Accepted: 25 July 2016

extracts from membranes of Acholeplasma laidlawii A grown with different fatty acids have a nearly constant spontaneous curvature. *Biochim. Biophys. Acta* **1257**, 18–24. (doi:10.1016/0005-2760(95)00042-B)

28. Parsons, J. B. & Rock, C. O. 2013 Bacterial lipids: metabolism and membrane homeostasis. *Prog. Lipid Res.* **52**, 249–276. (doi:10.1016/j.plipres.2013.02.002)

29. Hermansson, M., Hokynar, K. & Somerharju, P. 2011 Progress in Lipid Research Mechanisms of glycerophospholipid homeostasis in mammalian cells. *Prog. Lipid Res.* **50**, 240–257. (doi:10.1016/j.plipres.2011.02.004)

30. Yeung, T., Gilbert, G. E., Shi, J., Silvius, J., Kapus, A. & Grinstein, S. 2008 Membrane Phosphatidylserine Regulates Surface Charge and Protein Localization. *Science (80-.).* **319**, 210–213.

31. Baenke, F., Peck, B., Miess, H. & Schulze, A. 2013 Hooked on fat: the role of lipid synthesis in cancer metabolism and tumour development. *Dis. Model. Mech.* **6**, 1353–1363. (doi:10.1242/dmm.011338)

32. Pietiläinen, K. H. et al. 2011 Association of lipidome remodeling in the adipocyte membrane with acquired obesity in humans. *PLoS Biol.* **9**, e1000623. (doi:10.1371/journal.pbio.1000623)

33. Paolo, G. Di & Kim, T. 2011 Linking Lipids to Alzheimer ' s Disease : Cholesterol and Beyond. *Nat Rev Neurosci* **12**, 284–296. (doi:10.1038/nrn3012.Linking)

34. Li, Z., Agellon, L. B. & Vance, D. E. 2005 Phosphatidylcholine homeostasis and liver failure. *J. Biol. Chem.* **280**, 37798–37802. (doi:10.1074/jbc.M508575200)

35. Weijers, R. N. M. 2012 Lipid composition of cell membranes and its relevance in type 2 diabetes mellitus. *Curr. Diabetes Rev.* **8**, 390–400. (doi:10.2174/157339912802083531)

36. Attard, G. S., Templer, R. H., Smith, W. S., Hunt, A. N. & Jackowski, S. 2000 Modulation of CTP:phosphocholine cytidylyltransferase by membrane curvature elastic stress. *Proc. Natl. Acad. Sci. U. S. A.* **97**, 9032–9036. (doi:10.1073/pnas.160260697)

37. Cornell, R. B. & Arnold, R. S. 1996 Modulation of the activities of enzymes of membrane lipid metabolism by non-bilayer-forming lipids. *Chem. Phys. Lipids* **81**, 215–227. (doi:10.1016/0009-3084(96)02584-4)

38. Ces, O. & Mulet, X. 2006 Physical coupling between lipids and proteins: a paradigm for cellular control. *Signal Transduct.* **6**, 112–132. (doi:10.1002/sita.200500079)

39. Beard, J., Attard, G. S. & Cheetham, M. J. 2008 Integrative feedback and robustness in a lipid biosynthetic network. *J. R. Soc. Interface* **5**, 533–543. (doi:10.1098/rsif.2007.1155)

40. Dymond, M. K., Attard, G. S. & Postle, A. D. 2008 Testing the hypothesis that amphiphilic antineoplastic lipid analogues act through reduction of membrane curvature elastic stress. *J. R. Soc. Interface* **5**, 1371–1386.

41. Dymond, M. K. & Attard, G. S. 2008 Cationic type I amphiphiles as modulators of

Received: 21 March 2016
Accepted: 25 July 2016

membrane curvature elastic stress in vivo. *Langmuir* **24**, 11743–11751. (doi:10.1021/la8017612)

42. Cybulski, L. E., Martín, M., Mansilla, M. C., Fernández, A. & De Mendoza, D. 2010 Membrane thickness cue for cold sensing in a bacterium. *Curr. Biol.* **20**, 1539–1544. (doi:10.1016/j.cub.2010.06.074)

43. Lockshon, D., Olsen, C. P., Brett, C. L., Chertov, A., Merz, A. J., Lorenz, D. A., Van Gilst, M. R. & Kennedy, B. K. 2012 Rho signaling participates in membrane fluidity homeostasis. *PLoS One* **7**, 1–10. (doi:10.1371/journal.pone.0045049)

44. Zhang, X. H., Zhao, C. & Ma, Z. A. 2007 The increase of cell-membranous phosphatidylcholines containing polyunsaturated fatty acid residues induces phosphorylation of p53 through activation of ATR. *J. Cell Sci.* **120**, 4134–43. (doi:10.1242/jcs.015834)

45. Ye, J. & DeBose-Boyd, R. A. 2011 Regulation of cholesterol and fatty acid synthesis. *Cold Spring Harb. Perspect. Biol.* **3**, a004754–a004754. (doi:10.1101/cshperspect.a004754)

46. Dymond, M. K., Hague, C. V, Postle, A. D. & Attard, G. S. 2013 An in vivo ratio control mechanism for phospholipid homeostasis: evidence from lipidomic studies. *J. R. Soc. Interface* **10**, 20120854. (doi:10.1098/rsif.2012.0854)

47. Hague, C. V., Postle, A. D., Attard, G. S. & Dymond, M. K. 2013 Cell cycle dependent changes in membrane stored curvature elastic energy: evidence from lipidomic studies. *Faraday Discuss.* **161**, 481–497. (doi:10.1039/c2fd20078c)

48. In press. The LIPID MAPS Lipidomics Gateway, http://www.lipidmaps.org/.

49. Raetz, C. R. H. et al. 2006 Kdo2-Lipid A of Escherichia coli, a defined endotoxin that activates macrophages via TLR-4. *J. Lipid Res.* **47**, 1097–1111. (doi:10.1194/jlr.M600027-JLR200)

50. Dennis, E. A. et al. 2010 A Mouse Macrophage Lipidome. *J. Biol. Chem.* **285**, 39976–39985. (doi:10.1074/jbc.M110.182915)

51. Sampaio, J. L., Gerl, M. J., Klose, C., Ejsing, C. S., Beug, H., Simons, K. & Shevchenko, A. 2011 Membrane lipidome of an epithelial cell line. *Proc. Natl. Acad. Sci. U. S. A.* **108**, 1903–7. (doi:10.1073/pnas.1019267108)

52. Chan, R. B., Oliveira, T. G., Cortes, E. P., Honig, L. S., Duff, K. E., Small, S. A., Wenk, M. R., Shui, G. & Di Paolo, G. 2012 Comparative lipidomic analysis of mouse and human brain with Alzheimer disease. *J. Biol. Chem.* **287**, 2678–2688. (doi:10.1074/jbc.M111.274142)

53. Marsh, D. 2013 *Handbook of lipid bilayers*. CRC Press.

54. Lafleur, M., Bloom, M., Eikenberry, E. F., Gruner, S. M. & Cullis, P. R. 1996 Correlation between lipid plane curvature and lipid chain order. *Biophys J.* **70**, 2747–2757.

55. Leikin, S., Kozlov, M., Fuller, N. & Rand, R. 1996 Measured effects of diacylglycerol on structural and elastic properties of phospholipid membranes. *Biophys. J.* **71**, 2623–2632.

Received: 21 March 2016
Accepted: 25 July 2016

56. Kollmitzer, B., Heftberger, P., Rappolt, M. & Pabst, G. 2013 Monolayer spontaneous curvature of raft-forming membrane lipids. *Soft Matter* **9**, 10877. (doi:10.1039/c3sm51829a)

57. Chen, C. M. 2000 Theory for the bending rigidity of protein-coated lipid membranes. *Physica A* **281**, 41–50. (doi:10.1016/S0378-4371(00)00037-6)

58. Kaiser, H.-J., Lingwood, D., Levental, I., Sampaio, J. L., Kalvodova, L., Rajendran, L. & Simons, K. 2009 Order of lipid phases in model and plasma membranes. *Proc. Natl. Acad. Sci. U. S. A.* **106**, 16645–16650. (doi:10.1073/pnas.0908987106)

59. Dawaliby, R., Trubbia, C., Delporte, C., Noyon, C., Ruysschaert, J.-M., Van Antwerpen, P. & Govaerts, C. 2015 Phosphatidylethanolamine is a key regulator of membrane fluidity in eukaryotic cells. *J. Biol. Chem.* , jbc.M115.706523. (doi:10.1074/jbc.M115.706523)

60. Gibellini, F. & Smith, T. K. 2010 The Kennedy pathway-De novo synthesis of phosphatidylethanolamine and phosphatidylcholine. *IUBMB Life* **62**, 414–28. (doi:10.1002/iub.337)

61. Lands, W. E. M. 1957 Metabolism of Glycerolipides: A comparison of Lecithin and Triglceride Synthesis. *J. Biol. Chem.* , 883–889.

62. Yamashita, A., Hayashi, Y., Nemoto-Sasaki, Y., Ito, M., Oka, S., Tanikawa, T., Waku, K. & Sugiura, T. 2014 Acyltransferases and transacylases that determine the fatty acid composition of glycerolipids and the metabolism of bioactive lipid mediators in mammalian cells and model organisms. *Prog. Lipid Res.* **53**, 18–81. (doi:10.1016/j.plipres.2013.10.001)

63. Sadasivam, S., Duan, S. & DeCaprio, J. A. 2012 The MuvB complex sequentially recruits B-Myb and FoxM1 to promote mitotic gene expression. *Genes Dev.* **26**, 474–89. (doi:10.1101/gad.181933.111)

Dymond MK. 2016 J. R. Soc. Interface 13: 20160228. http://dx.doi.org/10.1098/rsif.2016.0228

Received: 21 March 2016
Accepted: 25 July 2016

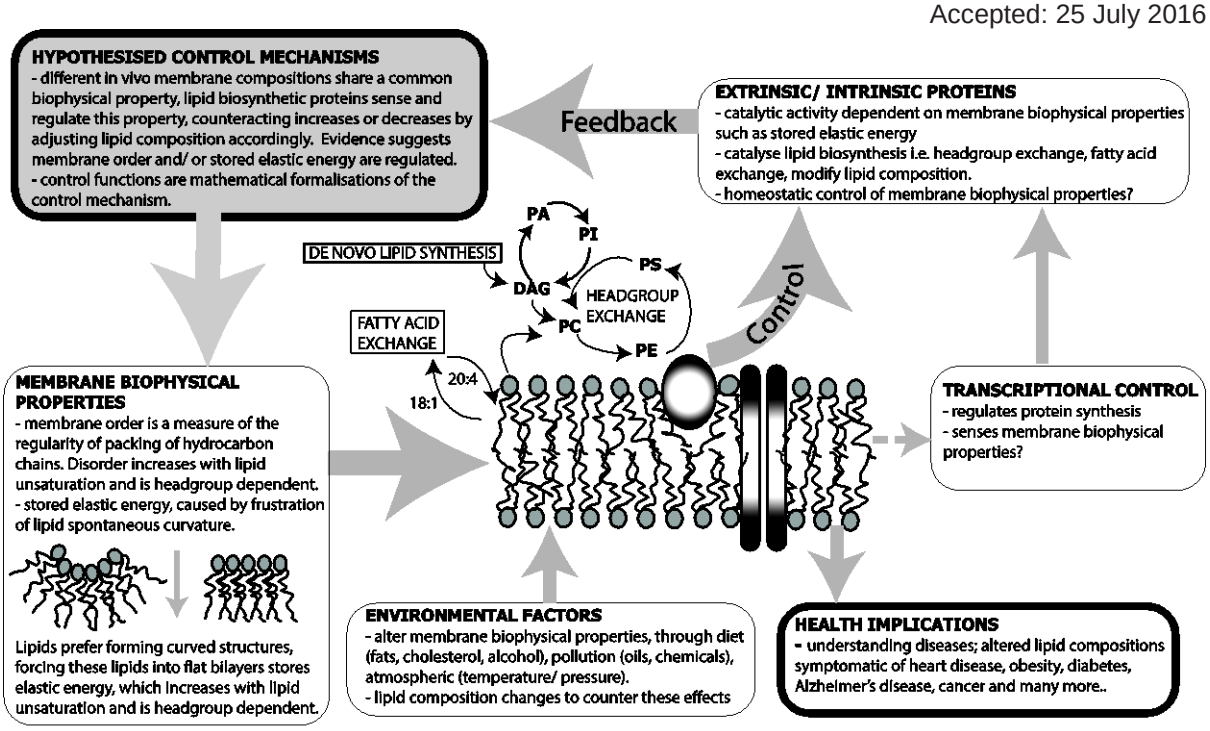

Figure 1 a schematic overview of how homeostatic control mechanisms might occur in phospholipid biosynthesis, showing the biophysical concepts of membrane order, spontaneous curvature and stored elastic energy. A simplified phospholipid biosynthetic pathway, where PC, PE, PI, PA, PS and DAG are phosphatidylcholine, phosphatidylethanolamine, phosphatidylinositol, phosphatidic acid, phosphatidylserine and diacylglycerol lipids respectively, is also shown. Membrane bound proteins involved in lipid biosynthesis, which can sense and regulate the biophysical properties of the membrane, the environmental contributions to lipid composition and health implications of understanding lipid biosynthesis are also summarised.

Dymond MK. 2016 J. R. Soc. Interface 13: 20160228. http://dx.doi.org/10.1098/rsif.2016.0228

Received: 21 March 2016
Accepted: 25 July 2016

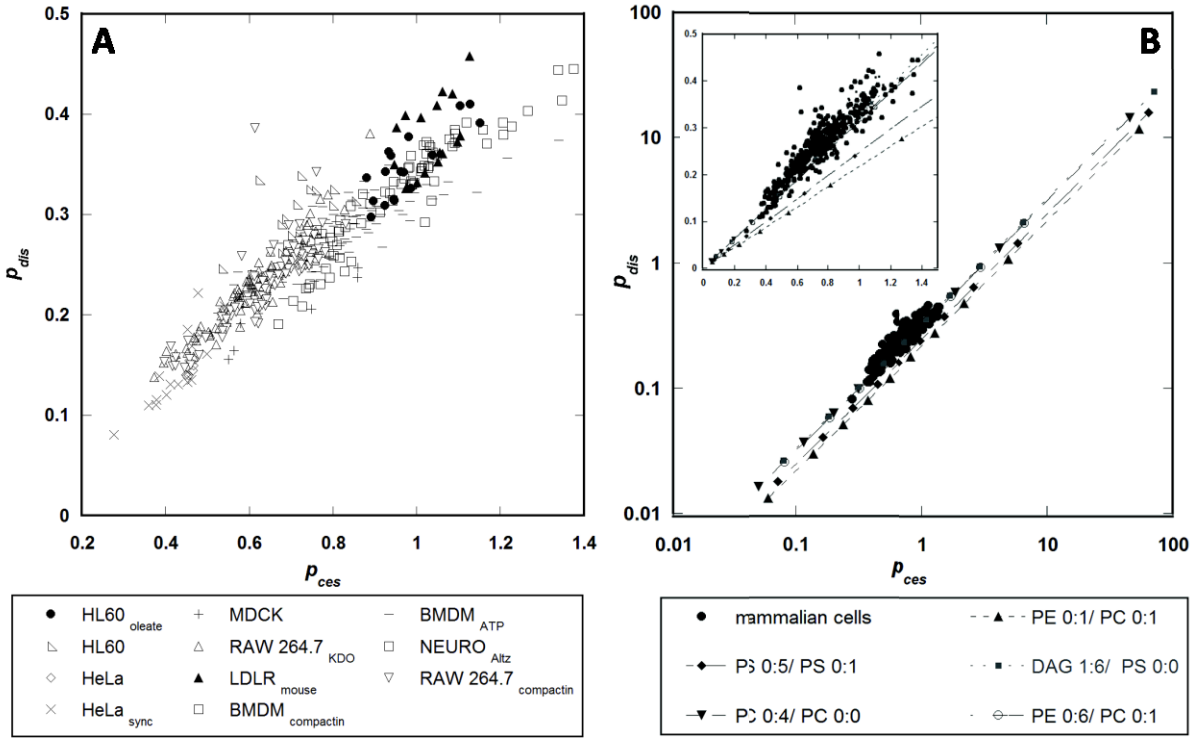

Figure 2A a plot of p_{dis} versus p_{ces} for around 500 individual cell populations derived from the cell lines summarised in Table 1. The Pearson correlation coefficient for the total data is 0.93 indicating that p_{dis} and p_{ces} are positively correlated. Figure 2B shows p_{dis} versus p_{ces} on a logarithmic scale calculated for a range of binary lipid mixtures (with increasing amounts of 10 mol% of the second lipid in the mixture) and the clustering of the p_{ces} and p_{dis} values determined for the mammalian cells shown in Figure 2A. The inset in Figure 2B shows the region where the mammalian cells cluster expanded and on a linear scale.

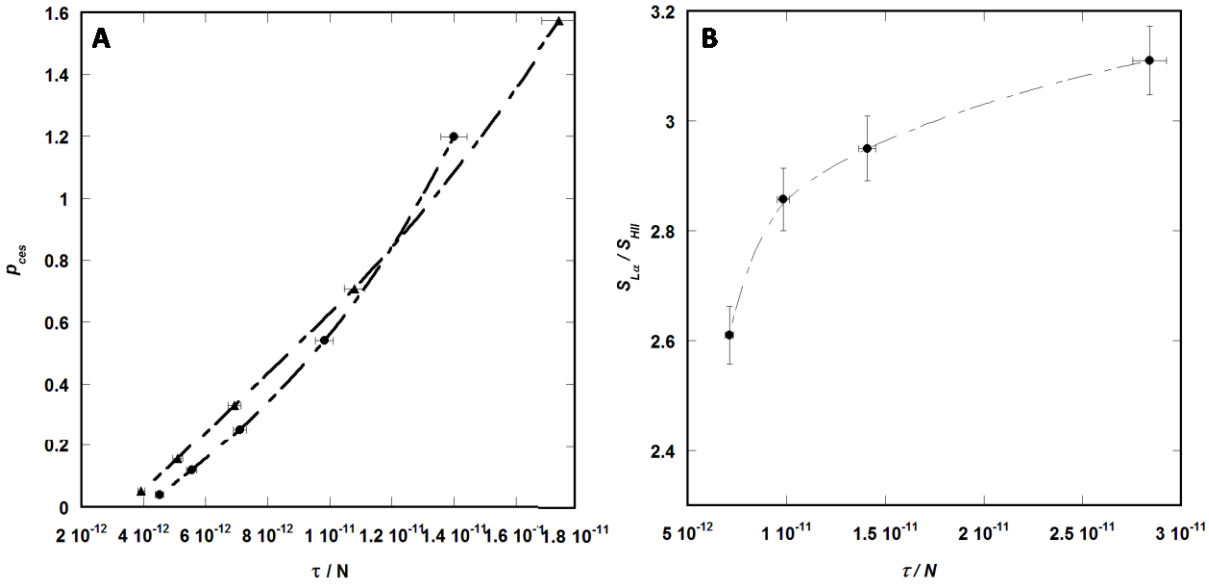

Dymond MK. 2016 J. R. Soc. Interface 13: 20160228. http://dx.doi.org/10.1098/rsif.2016.0228

Received: 21 March 2016
Accepted: 25 July 2016

Figure 3A the variance of p_{ces} with curvature elastic stress (τ) in binary POPC: POPE (black circles) or POPC: DOG (black triangles) lipid vesicles. Figure 3B curvature elastic stress versus $S_{L\alpha}$/ S_{LHII} in binary POPC: POPE (black circles) order parameter data taken from Lafleur et al. [54].

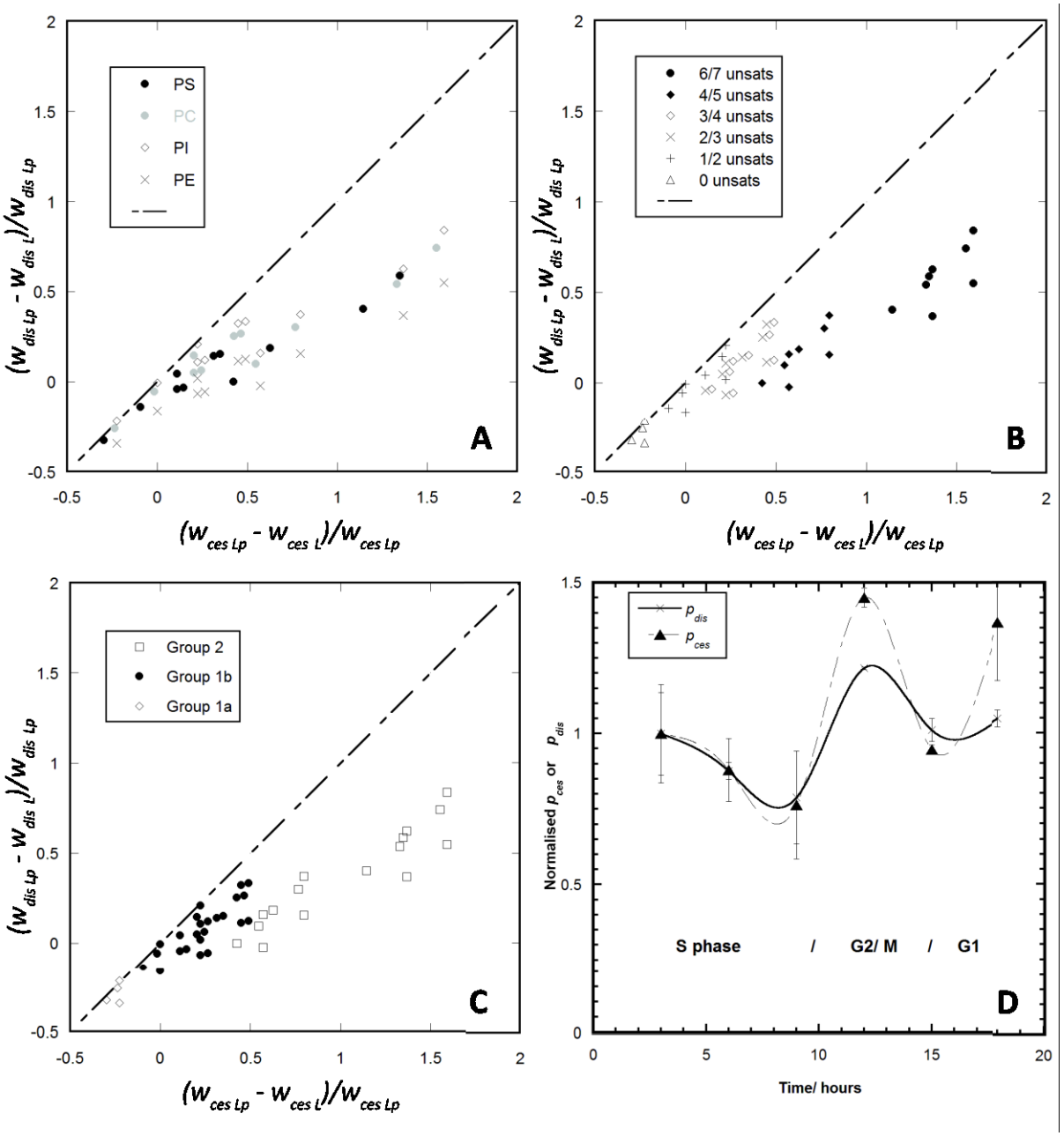

Figure 4 plots of $(w_{ces\ Lp} - w_{ces\ L})/ w_{ces\ Lp}$ versus $(w_{dis\ Lp} - w_{dis\ L})/ w_{dis\ Lp}$ showing how changes in the lipid composition of a dataset will impact each control function relative to the pivot species. Lipid species that fall on the line of equality (or close to it) have roughly equal effects on the magnitude of p_{ces} and p_{dis}. Figure 4A shows the lipids classified by headgroup

Received: 21 March 2016
Accepted: 25 July 2016

identity. Figure 4B shows the lipids classified by the total number of unsaturations in both hydrocarbon chains. Figure 4C shows the lipids classified into three groups (*Groups 1a, 1b and 2*) as discussed in the text. Figure 4D shows the relative changes in p_{ces} and p_{dis} about the cell cycle of the HeLa cell; p_{ces} data were normalised to the p_{ces} value at 3hours and p_{dis} data were normalised to the p_{dis} value at 3 hours. G1, S, G2 and M are the Gap 1, Synthesis, Gap 2 and Mitosis phases respectively and x-axis is the number of hours after the release of cells from synchronisation agent [47]. Increases in p_{ces} over p_{dis} during G2/M are driven by compositional increases in polyunsaturated lipids.

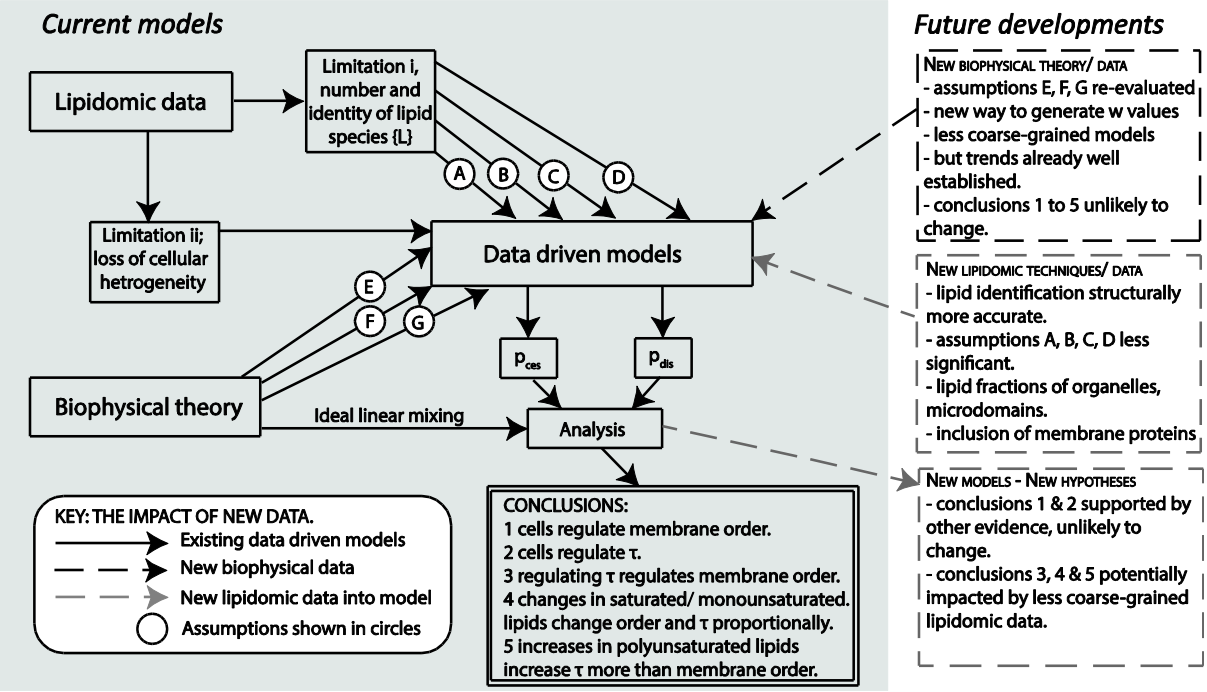

Figure 5, a summary of assumptions used to generate data-driven models and the impact of new lipidomic and/ or biophysical data on the conclusions of this manuscript.

Dymond MK. 2016 J. R. Soc. Interface 13: 20160228. http://dx.doi.org/10.1098/rsif.2016.0228

Received: 21 March 2016
Accepted: 25 July 2016

Table 1 mean values of p_{dis} and p_{ces} and the resultant c_v values for the different mammalian cell line lipidomes summarised *in sections 2.1 to 2.3*.

Cell Line		n	Mean	S_{dev}	$c_{v\,/\,\%}$	Mean (p_{dis}/p_{ces})	S_{dev} (p_{dis}/p_{ces})
HL60 $_{oleate}$	P_{dis}	17	0.98	0.08	8.38	2.82	0.16
	P_{ces}		0.35	0.03	9.89		
HL60	P_{dis}	16	0.71	0.07	10.46	2.42	0.25
	P_{ces}		0.30	0.03	10.89		
HeLa	P_{dis}	8	0.46	0.01	1.95	3.01	0.23
	P_{ces}		0.15	0.01	9.49		
LDLR $_{mouse}$	P_{dis}	16	1.04	0.06	5.36	2.75	0.23
	P_{ces}		0.38	0.04	9.65		
BMDM $_{ATP}$	P_{dis}	87	0.82	0.14	17.46	2.92	0.26
	P_{ces}		0.28	0.04	13.19		
RAW 264.7 $_{compactin}$	P_{dis}	116	0.64	0.09	14.79	2.79	0.20
	P_{ces}		0.23	0.04	17.26		
BMDM $_{compactin}$	P_{dis}	87	0.92	0.18	19.40	2.92	0.19
	P_{ces}		0.31	0.05	17.52		
RAW 264.7 $_{KDO}$	P_{dis}	96	0.60	0.10	15.95	2.69	0.15
	P_{ces}		0.23	0.04	17.99		
HeLa $_{sync}$ *	P_{dis}	18	0.44	0.07	16.30	3.01	0.39
	P_{ces}		0.15	0.04	26.65		
MDCK **	P_{dis}		0.69	0.15	21.24	3.45	0.22
	P_{ces}		0.20	0.04	18.59		
NEURO $_{Altz}$**	P_{dis}		0.75	0.05	6.92	3.35	0.13
	P_{ces}		0.23	0.02	10.20		

* These cells are synchronised at the G1/ S boundary

** The lipidome of these cells is reported as an average of 3 repeats

Dymond MK. 2016 J. R. Soc. Interface 13: 20160228. http://dx.doi.org/10.1098/rsif.2016.0228

Received: 21 March 2016
Accepted: 25 July 2016

Supplementary info for: Mammalian phospholipid homeostasis: evidence that membrane curvature elastic stress drives homeoviscous adaptation *in vivo*

Marcus K. Dymond*[1]

Division of Chemistry, School of Pharmacy and Biological Sciences, University of Brighton, BN2 4GL

*Author for correspondence: M.Dymond@brighton.ac.uk

Dymond MK. 2016 J. R. Soc. Interface 13: 20160228. http://dx.doi.org/10.1098/rsif.2016.0228

Received: 21 March 2016
Accepted: 25 July 2016

SI 1.1 A brief discussion of the effect of lipid composition on the variance of p_{ces} and p_{dis}

Table S3 shows the top 15 most compositionally abundant phospholipids in the lipidomes studied. If these lipidomes are not compositionally different to those already studied i.e. HeLa and HL60 then the novelty of these new results is low. The compositional diversity of the lipidomes is briefly discussed and the effect on p_{dis} and p_{ces} considered.

In the HL60 cell line the most abundant lipid is PE18:1/ 18:1, which is present at 8.0 % of the total lipids in the control function. A number of polyunsaturated PE lipids, such as PE 18:0/ 22:6 (4.7 %) and PE18:0/ 20:4 (7.0 %) are in the highest ten most abundant lipids. PC16:0/ 18:1 is the third most abundant lipid at 6.3% and PC 18:1/18:1 has 3.7 % abundance. Culturing the HL60 cell line with exogenous oleate (HL60 $_{oleate}$) causes PE18:1/18:1 to rise to 21.4% of the total lipid analysed. PC 18:1/18:1 also rises to 7.5%, polyunsaturated PE lipids remain prevalent in the ten most abundant species but surprisingly DAG 18:1/18:1, not apparent in highest 15 abundant lipids in the HL60 lipidome, is now at 4.34 % abundance. In the HeLa cell line the most abundant lipid is PC 16:0/18:1 (12.1 %) followed by PE 18:1/18:1 (9.7%). Monounsaturated and diunsaturated PC and PE lipids dominate the lipidome with some polyunsaturated PE lipids (PE 18:0/ 20:4 and PE 18:1/20:4) present. The c_v values of p_{dis}, p_{ces} for HL60$_{oleate}$, HL60 and HeLa cell lines (reproduced from our previous publications [1,2]) are close to or below 10%.

The LDLR $_{mouse}$ lipidome is determined from thioglycolate-stimulated wild-type and low-density lipoprotein receptor knockout (LDLR(-/-)) mice [3] maintained on normal and Western (High-fat, high cholesterol) diets. The lipids PS(36:1), PS(36:2) and PS(38:8) dominate the composition at 6.1 %, 5.4 % and 3.7 % respectively, polyunsaturated PS, PE, PC and a PI are also common. PC(36:2) is the highest dominating PC lipid at 2.2 % of the total phospholipid composition. The mean c_v of p_{dis} and p_{ces} are 5.36% and 9.65% respectively, giving excellent evidence that both control functions are in operation across a range of control and experimental studies.

In RAW 264.7 cells, cultured with KDO lipid-A and/ or ATP. (RAW 264.7$_{KDO}$) [3–5], PS(36:1) at 6.8 % is the most abundant lipid. PC(36:2) is the second most abundant at 3.2 %. Polyunsaturated PE, PS and PI lipids are also abundant but polyunsaturated PC lipids are not

Received: 21 March 2016
Accepted: 25 July 2016

present (Table S3). The mean c_v of p_{dis} and p_{ces} are 17.46% and 13.19% respectively. Similar values of the mean c_v of p_{dis} and p_{ces} were obtained for RAW 264.7 cells, cultured with compactin (RAW $264.7_{compactin}$)[3–5] and BMDM cells treated with compactin or ATP (BMDM $_{compactin}$ and BMDM $_{ATP}$, respectively) [3,5]. In the BMDM $_{ATP}$ experiments the most abundant lipids are PS(36:1) at 7.2 %, PC(36:2) at 3.4 %, PC(34:1) at 3.86 % and PE(36:2) at 3.4 %. The BMDM $_{compactin}$ experiments show a similar composition to the BDM $_{ATP}$ lipidome, except that in the BMDM $_{compactin}$ lipidome polyunsaturated PC lipids such as PC(40:7) is now the third most dominant lipid at 3.9%.

The lipidome of MDCK cells [6] is dominated by PC (34:1) at 9.8 % and PS(36:1)at 5.9 %, Table S3. The c_v of p_{dis} and p_{ces} for the MDCK cell line are 18.59 % and 21.24 respectively. Finally, the lipidome of human brain cells exhibiting Alzheimer's Disease and control (NEURO $_{Alz}$) [7] is dominated by the PC lipids PC(34:1) at 12.5%, PC(32:0) at 8.1% and PC(36:1) at 5.6%, this is the only cell line with a dominant saturated lipid species at such high composition. The c_v of p_{dis} and p_{ces} for these lipidomes are 6.92 and 10.2 % respectively. We conclude in the manuscript that there is good evidence for the previously identified control mechanisms operating in these new cell lines since general p_{ces} and p_{dis} are in the range of 5 to 20%.

Dymond MK. 2016 J. R. Soc. Interface 13: 20160228. http://dx.doi.org/10.1098/rsif.2016.0228

Received: 21 March 2016
Accepted: 25 July 2016

Supplementary Figures

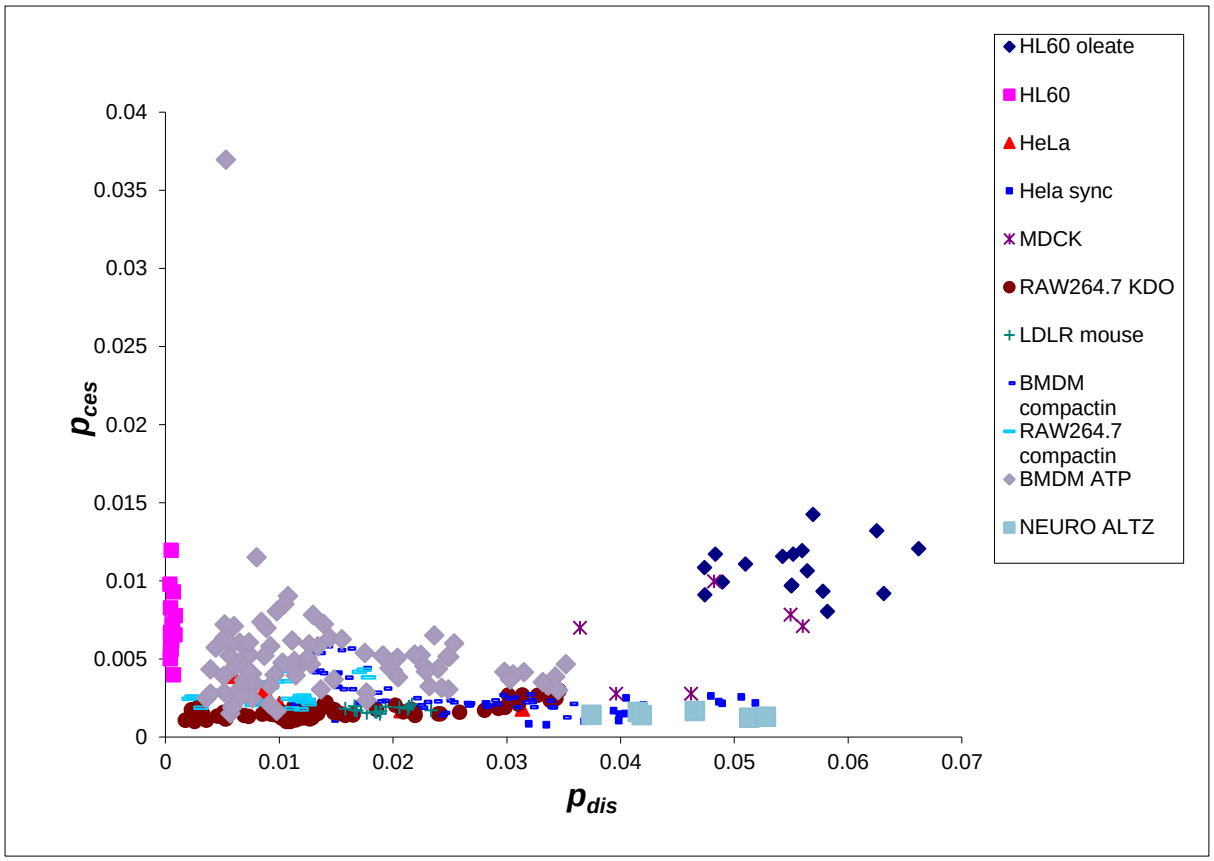

Figure S1; a correlation plot of p_{ces} and p_{dis} constructed using w_{ces} and w_{dis} parameter sets previously discarded since they showed gave low variance across the HL60 and HeLa cell populations studies [1,2].

Dymond MK. 2016 J. R. Soc. Interface 13: 20160228. http://dx.doi.org/10.1098/rsif.2016.0228

Received: 21 March 2016
Accepted: 25 July 2016

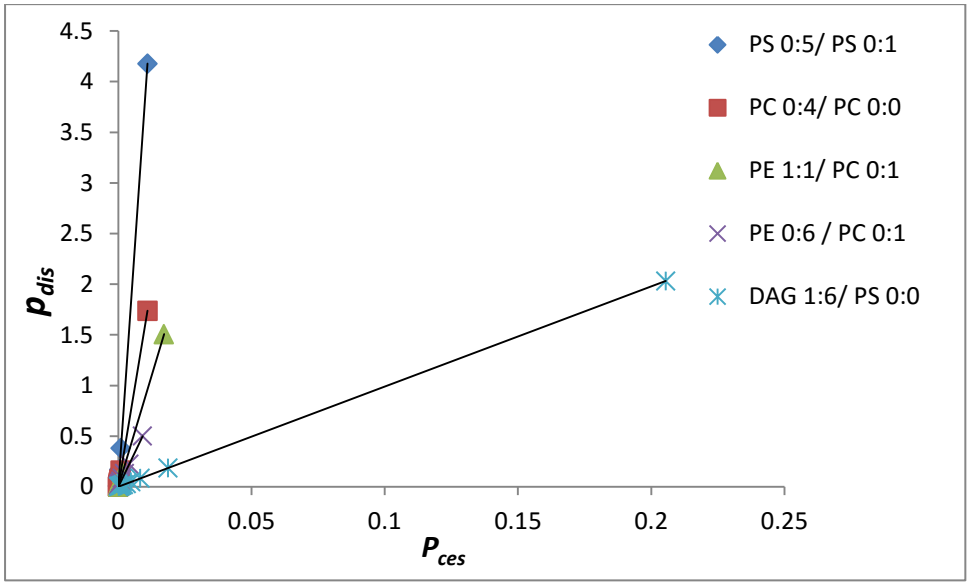

Figure S2 p_{ces} and p_{dis} calculated for binary lipid mixtures using the same previously discarded parameter sets as for Figure S1.

S1.2 Construction of the calibration plot relating p_{ces} to curvature elastic stress

We accomplish this using the addition rule for spontaneous curvatures based on the principle of ideal mixing as discussed [8]. Where;

$$c_{0\,mix} = (1\text{-}x)\, c_{0\,A} + x c_{0\,B} \qquad \text{Eq. S1,}$$

such that $c_{0\,mix}$ is the spontaneous curvature of a mixture of lipids A and B, x is the mole fraction of lipid B and C_{0A} and C_{0B} are the spontaneous curvatures of the pure lipids A and B.

Curvature elastic stresses are calculated using Eq. 3, main manuscript, using c_{0mix} and a κ_{Mmix} term. Typical values of κ_M for pure lipid monolayers are of the order of $0.5\text{x}10^{-19}$ J for DOPE [9] and DOG [10] whilst for DOPC $1.0\text{x}10^{-19}$ J is reported [9]. We use a similar addition rule (Eq. S1) to calculate κ_{Mmix} for these mixtures. It should however be noted that, in comparison to the range of spontaneous curvature values of lipids, κ_M varies only slightly indicating that the principal contribution to curvature elastic stress is the frustrated lipid spontaneous curvature.

Dymond MK. 2016 J. R. Soc. Interface 13: 20160228. http://dx.doi.org/10.1098/rsif.2016.0228

Received: 21 March 2016
Accepted: 25 July 2016

Table S4 enzymes with acyl glycerol transferase activity as discussed [11]. The presence of individual transcripts was assessed by looking through data for GSE 26922, from the Gene Expression Omnibus [12].

AGPAT 9, AGPAT3, AGPAT1, AGPAT2, AGPAT6, AGPAT5, AGPAT4, AGPAT9, LPGAT1, GPAT2, AGPAT3, AGPAT2, AGPAT6, AGPAT4, AGPAT5, ABHD5, PNPLA2, PNPLA4, PNPLA2, PNPLA6, PNPLA2, PNPLA1, PNPLA7, DGAT2, MBOAT1, MBOAT2, MBOAT4, MBOAT7,LPCAT1, LPCAT2, LPCAT3, LPCAT4, PLA1, LPA1, PLA2, PLA2 GROUP IVB, PLA2 GROUP III, PLA GROUPIVF, PLA GROUPVI, PLA GROUPIIC, PLA GROUPIIF, PLA GROUPX, PLA GROUPIVD, PLA GROUPXV, PLA GROUPXVI, PLA GROUPVII, PLA GROUPIVA, PLA GROUPIIA, PLA GROUPIID, PLA GROUPVIIB, PLA GROUPVIIA, LYPLA2, PLA GROUPIIE, PLA GROUPIII.

References

1. Dymond, M. K., Hague, C. V, Postle, A. D. & Attard, G. S. 2013 An in vivo ratio control mechanism for phospholipid homeostasis: evidence from lipidomic studies. *J. R. Soc. Interface* **10**, 20120854. (doi:10.1098/rsif.2012.0854)

2. Dymond, M. K. 2015 Mammalian phospholipid homeostasis: Homeoviscous adaptation deconstructed by lipidomic data driven modelling. *Chem. Phys. Lipids* **191**, 136–146. (doi:10.1016/j.chemphyslip.2015.09.003)

3. In press. The LIPID MAPS Lipidomics Gateway, http://www.lipidmaps.org/.

4. Dennis, E. a et al. 2010 A mouse macrophage lipidome. *J. Biol. Chem.* **285**, 39976–85. (doi:10.1074/jbc.M110.182915)

5. Raetz, C. R. H. et al. 2006 Kdo2-Lipid A of Escherichia coli, a defined endotoxin that activates macrophages via TLR-4. *J. Lipid Res.* **47**, 1097–1111. (doi:10.1194/jlr.M600027-JLR200)

6. Sampaio, J. L., Gerl, M. J., Klose, C., Ejsing, C. S., Beug, H., Simons, K. & Shevchenko, A. 2011 Membrane lipidome of an epithelial cell line. *Proc. Natl. Acad. Sci. U. S. A.* **108**, 1903–7. (doi:10.1073/pnas.1019267108)

Received: 21 March 2016
Accepted: 25 July 2016

7. Chan, R. B., Oliveira, T. G., Cortes, E. P., Honig, L. S., Duff, K. E., Small, S. A., Wenk, M. R., Shui, G. & Di Paolo, G. 2012 Comparative lipidomic analysis of mouse and human brain with Alzheimer disease. *J. Biol. Chem.* **287**, 2678–2688. (doi:10.1074/jbc.M111.274142)

8. Marsh, D. 1996 Intrinsic curvature in normal and inverted lipid structures and in membranes. *Biophys. J.* **70**, 2248–55. (doi:10.1016/S0006-3495(96)79790-4)

9. Marsh, D. 2006 Elastic curvature constants of lipid monolayers and bilayers. *Chem. Phys. Lipids* **144**, 146–159. (doi:10.1016/j.chemphyslip.2006.08.004)

10. Leikin, S., Kozlov, M., Fuller, N. & Rand, R. 1996 Measured effects of diacylglycerol on structural and elastic properties of phospholipid membranes. *Biophys. J.* **71**, 2623–2632.

11. Yamashita, A., Hayashi, Y., Nemoto-Sasaki, Y., Ito, M., Oka, S., Tanikawa, T., Waku, K. & Sugiura, T. 2014 Acyltransferases and transacylases that determine the fatty acid composition of glycerolipids and the metabolism of bioactive lipid mediators in mammalian cells and model organisms. *Prog. Lipid Res.* **53**, 18–81. (doi:10.1016/j.plipres.2013.10.001)

12. Edgar, R., Domrachev, M. & Lash, A. E. 2002 Gene Expression Omnibus: NCBI gene expression and hybridization array data repository. *Nucleic Acids Res.* **30**, 207–10. (doi:10.1093/nar/30.1.207)

Table S1 the w_{ces} values of lipids used to parameterise Equation 1 and calculate p_{ces} *

Unsats C1 \ Unsats C2	PS w_{ces} values						
	0	1	2	3	4	5	6
0	0.2204	0.2842	0.348	0.3596	0.4466	0.5626	0.6728
1		0.348	0.4118	0.4234	0.5104	0.6264	0.7366
2			0.4756	0.4872	0.5742	0.6902	0.8004
3				0.4988	0.5858	0.7018	0.812
4					0.6728	0.7888	0.899
5						0.9048	1.015
6							1.1252

Unsats C1 \ Unsats C2	PC w_{ces} values						
	0	1	2	3	4	5	6
0	0.2394	0.3087	0.378	0.3906	0.4851	0.6111	0.7308
1		0.378	0.4473	0.4599	0.5544	0.6804	0.8001
2			0.5166	0.5292	0.6237	0.7497	0.8694
3				0.5418	0.6363	0.7623	0.882
4					0.7308	0.8568	0.9765
5						0.9828	1.1025
6							1.2222

Unsats C1 \ Unsats C2	PI w_{ces} values						
	0	1	2	3	4	5	6
0	0.2432	0.3136	0.384	0.3968	0.4928	0.6208	0.7424
1		0.384	0.4544	0.4672	0.5632	0.6912	0.8128
2			0.5248	0.5376	0.6336	0.7616	0.8832
3				0.5504	0.6464	0.7744	0.896
4					0.7424	0.8704	0.992
5						0.9984	1.12
6							1.2416

Unsats C1 \ Unsats C2	PE w_{ces} values						
	0	1	2	3	4	5	6
0	0.2432	**0.3136**	0.384	0.3968	0.4928	0.6208	0.7424
1		0.384	0.4544	0.4672	0.5632	0.6912	0.8128
2			0.5248	0.5376	0.6336	0.7616	0.8832
3				0.5504	0.6464	0.7744	0.896
4					0.7424	0.8704	0.992
5						0.9984	1.12
6							1.2416

Unsats C1 \ Unsats C2	PA w_{ces} values						
	0	1	2	3	4	5	6
0	0.2698	0.3479	0.426	0.4402	0.5467	0.6887	0.8236
1		0.426	0.5041	0.5183	0.6248	0.7668	0.9017
2			0.5822	0.5964	0.7029	0.8449	0.9798
3				0.6106	0.7171	0.8591	0.994
4					0.8236	0.9656	1.1005
5						1.1076	1.2425
6							1.3774

Unsats C1 \ Unsats C2	DAG w_{ces} values						
	0	1	2	3	4	5	6
0	0.3192	0.4116	0.504	0.5208	0.6468	0.8148	0.9744
1		0.504	0.5964	0.6132	0.7392	0.9072	1.0668
2			0.6888	0.7056	0.8316	0.9996	1.1592
3				0.7224	0.8484	1.0164	1.176
4					0.9744	1.1424	1.302
5						1.3104	1.47
6							1.6296

* where DAG, PA, PI, PE, PC, PS are the diacylglycerol, phosphatidic acid, phosphatidylinositol, phosphatidylethanolamine, phosphatidylcholine and phosphatidylserine headgroups. Commonly occuring lipids in the mammalian lipidome are shaded grey and the terms Unsats C1 and Unsats C2, refer to the number of unsaturations in the first and second hydrocarbon chain respectively. The value shown in bold is the pivot species PE 0:1 for the p_{ces} control function.

Table S2 the w_{dis} values of lipids used to parameterise Equation 1 and calculate p_{dis} *

Unsats C1 \ Unsats C2	PS w_{dis} values						
	0	1	2	3	4	5	6
0	0.5084	0.6478	0.7216	0.7298	**0.7544**	1.0004	1.0578
1		0.7872	0.861	0.8692	0.8938	1.1398	1.1972
2			0.9348	0.943	0.9676	1.2136	1.271
3				0.9512	0.9758	1.2218	1.2792
4					1.0004	1.2464	1.3038
5						1.4924	1.5498
6							1.6072

Unsats C1 \ Unsats C2	PC w_{dis} values						
	0	1	2	3	4	5	6
0	0.558	0.711	0.792	0.801	0.828	1.098	1.161
1		0.864	0.945	0.954	0.981	1.251	1.314
2			1.026	1.035	1.062	1.332	1.395
3				1.044	1.071	1.341	1.404
4					1.098	1.368	1.431
5						1.638	1.701
6							1.764

Unsats C1 \ Unsats C2	PI w_{dis} values						
	0	1	2	3	4	5	6
0	0.589	0.7505	0.836	0.8455	0.874	1.159	1.2255
1		0.912	0.9975	1.007	1.0355	1.3205	1.387
2			1.083	1.0925	1.121	1.406	1.4725
3				1.102	1.1305	1.4155	1.482
4					1.159	1.444	1.5105
5						1.729	1.7955
6							1.862

Unsats C1 \ Unsats C2	PE w_{dis} values						
	0	1	2	3	4	5	6
0	0.496	0.632	0.704	0.712	0.736	0.976	1.032
1		0.768	0.84	0.848	0.872	1.112	1.168
2			0.912	0.92	0.944	1.184	1.24
3				0.928	0.952	1.192	1.248
4					0.976	1.216	1.272
5						1.456	1.512
6							1.568

Unsats C1 \ Unsats C2	PA w_{dis} values						
	0	1	2	3	4	5	6
0	0.4774	0.6083	0.6776	0.6853	0.7084	0.9394	0.9933
1		0.7392	0.8085	0.8162	0.8393	1.0703	1.1242
2			0.8778	0.8855	0.9086	1.1396	1.1935
3				1.183987	0.9163	1.1473	1.2012
4					0.9394	1.1704	1.2243
5						1.4014	1.4553
6							1.5092

Unsats C1 \ Unsats C2	DAG w_{dis} values						
	0	1	2	3	4	5	6
0	0.6014	0.7663	0.8536	0.8633	0.8924	1.1834	1.2513
1		0.9312	1.0185	1.0282	1.0573	1.3483	1.4162
2			1.1058	1.1155	1.1446	1.4356	1.5035
3				1.1252	1.1543	1.4453	1.5132
4					1.1834	1.4744	1.5423
5						1.7654	1.8333
6							1.9012

* where DAG, PA, PI, PE, PC, PS are the diacylglycerol, phosphatidic acid, phosphatidylinositol, phosphatidylethanolamine, phosphatidylcholine and phosphatidylserine headgroups. Commonly occuring lipids in the mammalian lipidome are shaded grey and the terms Unsats C1 and Unsats C2, refer to the number of unsaturations in the first and second hydrocarbon chain respectively. The value shown in bold is the pivot species PS 0:4 for the p_{dis} control function.

Figure S3, percentage total molar phospholipid composition of the fifteen most abundant phospholipids in each lipidome.

HL60			HL60 $_{oleate}$			HeLa		
Mean	SD		Mean	SD		Mean	SD	
8.05	2.55	PE18:1/18:1	21.44	6.89	PE18:1/18:1	12.11	3.68	PC16:0/18:1
6.99	2.80	PE18:0/20:4	7.49	2.24	PC18:1/18:1	9.73	5.66	PE18:1/18:1
6.38	1.66	PC16:0/18:1	6.64	1.71	PC16:0/18:1	8.86	3.04	PC18:1/18:1
4.72	1.71	PE18:0/22:6	6.56	2.32	PE18:0/18:1	6.05	3.04	PE18:0/18:1
4.23	1.49	PE18:0/18:1	4.69	1.98	PE18:0/20:4	4.02	2.97	PE16:0/18:1
3.83	1.25	PE18:1/20:4	4.35	3.82	AG18:1/18:1	3.52	1.61	PC16:0a/18:1
3.73	0.60	PC16:0/16:1	4.29	1.73	PE18:1/20:4	2.96	0.71	PE18:0/20:4
3.65	0.96	PC18:1/18:1	3.48	1.31	PE18:0/22:6	2.96	1.00	PC18:0/18:1
3.62	0.69	PC16:1/18:1	2.46	0.78	PE16:0/18:1	2.74	1.02	PC16:0/16:1
2.75	0.66	PE16:0/18:1	2.18	0.97	PE18:0a/22:0	2.66	0.74	PE18:1/20:4
2.69	0.72	PE18:1/18:2	2.04	0.63	PE18:1/18:2	2.32	0.72	PC16:0/18:2
2.54	1.06	PE18:0/22:5	1.95	0.81	PE18:0/22:5	2.21	1.12	PE18:0/20:2
2.52	0.92	PE18:0a/22:0	1.71	0.70	PE18:0/20:2	1.88	0.64	PC16:0/16:0
2.02	0.54	PC18:1/18:2	1.64	0.34	PC16:0/18:2	1.78	0.67	PC18:0/20:2
1.76	0.86	PE18:0/20:3	1.54	0.25	PC16:0/16:1	1.72	0.74	PC18:0a/18:2

RAW 264.7 $_{KDO}$			RAW 264.7 $_{compactin}$			BMDM $_{ATP}$		
Mean	SD		Mean	SD		Mean	SD	
6.76	2.62	PS(36:1)	6.59	1.89	PC(36:2)	7.21	3.18	PS(36:1)
3.27	1.10	PC(36:2)	5.58	1.49	PC(32:1)	7.12	4.88	PC(36:2)
2.82	1.12	PS(40:5)	5.57	1.45	PS(36:1)	3.86	2.00	PC(34:1)
2.74	0.93	PC(36:1)	3.41	0.84	PC(34:1)	3.40	1.01	PE(36:2)
2.62	1.14	PS(34:1)	3.13	1.35	PC(36:1)	3.15	2.27	PC(36:1)
2.60	1.04	PE(38:4)	3.01	1.04	PE(38:4)	3.07	0.88	PE(38:4)
2.51	0.83	PC(32:1)	2.59	0.88	PE(36:2)	3.01	1.02	PE(36:1)
2.36	0.97	PS(40:6)	2.29	0.62	PE(36:1)	2.82	1.49	PC(32:1)
2.23	1.14	PS(36:0)	2.16	0.81	PS(34:1)	2.45	1.06	PS(36:2)
1.97	0.64	PE(36:1)	2.15	0.61	PC(34:2)	2.45	2.14	PC(38:6)
1.80	0.63	PE(36:2)	1.89	0.53	PE(38:5e)/PE(38:4p)	2.43	1.00	PS(38:4)
1.80	0.78	PI(38:4)	1.80	0.56	PC(38:4)	2.32	0.97	PS(34:1)
1.73	0.73	PI(38:3)	1.57	0.39	PS(36:2)	2.07	1.98	PC(40:6)
1.66	0.70	PS(36:2)	1.54	0.49	PE(38:5)	1.96	1.01	PE(38:5e)/PE(38:4p)
1.66	0.55	PE(34:1)	1.53	0.42	PE(34:1)	1.88	0.66	PS(40:6)

MDCK			**NEURO $_{Altz}$**			**LDLR $_{mouse}$**		
Mean	SD		Mean	SD		Mean	SD	
11.25	1.91	PC 34:1	12.50	1.22	PC 34:1	6.09	0.76	PS(36:1)
6.78	0.98	PS 18:0-18:1	8.13	1.18	PC 32:0	5.43	1.32	PS(36:2)
6.22	1.55	PC 36:2	5.56	0.44	PC 36:1	3.70	1.12	PS(38:4)
4.38	0.57	PC 34:2	5.05	1.85	PS 36:1	3.30	0.82	PE(38:4)
3.67	0.43	PC 32:1	4.97	1.26	PE 40:6	3.09	0.44	PS(34:1)
3.16	0.89	PE 18:1-18:1	4.46	1.00	PI 38:4	2.97	0.28	PI(38:4)
3.02	0.98	PE 18:0-18:1	3.70	0.83	PC 36:4	2.95	0.45	PE(38:5e)/PE(38:4p)
2.94	0.90	PI 18:0-20:4	3.58	0.81	PC 38:4	2.62	1.72	PS(40:4)
2.86	1.24	PE O-18:1-20:4	3.55	0.44	PC 34:0	2.19	0.92	PC(36:2)
2.76	1.02	PC 36:3	3.55	0.16	PC 36:2	2.18	0.30	PS(38:3)
2.43	0.50	PI 18:0-20:3	2.82	0.92	PS 40:6	1.95	0.40	PC(38:6)
2.42	0.88	PC 36:1	2.37	0.24	PC 32:1	1.92	0.54	PC(38:4)
2.05	0.93	PE O-18:1-18:1	2.20	0.17	PC 38:6	1.72	0.42	PC(36:1)
1.86	0.66	PI 18:0-18:1	2.14	0.44	PE 38:4	1.70	0.37	PS(40:5)
1.86	0.84	PC 36:4	1.91	0.32	PC 40:6	1.65	0.32	PC(38:5)

BMDM $_{compactin}$		
Mean	SD	
7.55	4.79	PS(36:1)
5.44	2.24	PC(36:2)
4.44	3.93	PC(40:7)
3.76	1.30	PC(32:1)
3.31	1.72	PC(36:1)
3.10	2.54	PC(40:6)
2.91	1.27	PC(34:1)
2.88	1.09	PE(36:2)
2.54	0.97	PE(36:1)
2.35	1.66	PC(38:5)
2.33	1.40	PS(36:2)
2.21	2.53	PE(40:7e)/PE(40:6p)
2.14	1.48	PC(38:6)
2.14	1.14	PS(34:1)
2.03	1.41	PC(38:4)